EVALUATION OF A CAMPTOTHECIN/SODIUM-R-ALPHA LIPOATE COMBINATION FOR THE TREATMENT OF NON-SMALL CELL LUNG CANCER

by

SHERIF IBRAHIM

A dissertation submitted to the

Graduate School-New Brunswick

Rutgers, The State University of New Jersey

In partial fulfillment of the requirements

For the degree of

Doctor of Philosophy

Graduate Program in Pharmaceutical Science

Written under the direction of

Dr. Patrick J. Sinko

And approved by

_____

_____

_____

_____

New Brunswick, New Jersey

JANUARY, 2015

ABSTRACT OF THE DISSERTATION

EVALUATION OF A CAMPTOTHECIN/SODIUM-R-ALPHA LIPOATE COMBINATION FOR THE TREATMENT OF NON-SMALL CELL LUNG CANCER

By SHERIF IBRAHIM

Dissertation Director:

Dr. Patrick J. Sinko

Lung cancer is the most common cause of cancer-related mortality among both men and women in the United States and worldwide, killing more people than breast, prostate, and colon cancers combined. It is estimated that 1.37 million people worldwide die of the disease annually. Non-small cell lung cancer (NSCLC) accounts for the majority of lung cancer cases worldwide and thus remains a primary focus of therapeutic lung cancer research. Currently used treatments for NSCLC include surgery, chemotherapy, radiotherapy, and targeted/biological therapy. Despite these treatment options, the disease remains a considerable cause of morbidity and mortality. Thus, more effective treatment options are highly sought after. NSCLC is most often diagnosed at late stages, at which time surgery can no longer offer a curative outcome. Thus, cytotoxic chemotherapy remains the first-line treatment for late-stage NSCLC. However, efficacy has been modest at best and toxicity remains a significant drawback. Improvements to current chemotherapeutic strategies are direly needed.

The objective of this thesis is to evaluate a combination of camptothecin (CPT) and sodium-R-alpha lipoate (Na-RALA) for the treatment of NSCLC. Using a variety of concentration- and time-dependent in vitro assays, we found that a combination of CPT and Na-RALA: 1) exerted additive/synergistic cytotoxic effects against A549 human NSCLC adenocarcinoma cells; 2) has higher efficacy, higher cancer-selectivity, and lower toxicity towards normal cells than CPT alone; 3) simultaneously targets multiple hallmarks of cancer, including migration, invasion, senescence, and angiogenesis, and thus has the potential to reduce metastasis and general progression of NSCLC. In vivo evaluation of the combination began with the development of an orthotopic xenograft NSCLC model. The intrathoracic (IT) and intracardiac (IC) mouse models of NSCLC were deemed most fitting for our study design and objectives. A combination of CPT and Na-RALA deserves further evaluation as a treatment for NSCLC.

DEDICATION

I dedicate this work to my parents, Eman and Hassan, who sacrificed everything for me. To my brother and best friend Ahmed. To my grandmother Houria and my uncle Mohamed, I miss you everyday and I wish you were here with me. I dedicate my work and my life to you all.

ACKNOWLEDGEMENT

I would like to thank Dr. Patrick J. Sinko for his mentorship and relentless support. I would also like to thank Dr. Dayuan Gao and Dr. Zoltan Szekely.

TABLE OF CONTENTS

LIST OF TABLES

LIST OF ILLUSTRATIONS

1. INTRODUCTION

Lung cancer is the leading cancer killer among men and women in the United States and worldwide, killing more people than breast, prostate, and colorectal cancers combined [1, 2]. It is estimated that 1.37 million people worldwide die of the disease annually. An estimated 159,260 Americans are expected to die from lung cancer in 2014, accounting for approximately 27% of all US cancer deaths. Non-small cell lung cancer (NSCLC) is by far the most prevalent type of lung cancer, accounting for nearly 85% of all lung cancer cases. With a 5-year survival rate of ~15% in the United States and ~8% in Europe and the developing world, NSCLC remains a highly lethal cancer [2]. Currently used treatments for the disease include surgery (the only potentially curative option), chemotherapy, radiotherapy, targeted/biological therapy, and multimodal therapy combining two or more of these treatments. Despite these treatment options, the general prognosis of NSCLC remains extremely poor. Early-stage NSCLC presents with vague and variable symptoms that are commonly overlooked by effected patients. For this reason, the majority of NSCLC cases are diagnosed at late stages during which surgery can no longer offer a curative outcome. Thus, cytotoxic chemotherapy with multiple agents remains the most common treatment in NSCLC patients. However, less-than-optimal efficacy and high treatment-related toxicity remain significant issues with this type of treatment. Thus, improvement to current standard-of-care chemotherapy for NSCLC is needed.

One potentially successful option currently under investigation is combination therapy with a cytotoxic chemotherapeutic agent(s) and a selective, non-cytotoxic agent, with the ultimate aim being the production of a more potent and more targeted

therapeutic effect. This type of combination therapy can have major advantages, including higher potency, higher cancer-selectivity, lower toxicity, and a potential for greatly reduced therapeutic doses. In fact, this is already being used clinically as seen with the combination of cytotoxic agents with targeted/biological agents. Examples include the addition of bevacizumab (Avastin®), an antibody targeting vascular endothelial growth factor (VEGF), to standard first-line combination chemotherapy [3].

Camptothecin (CPT) is a cytotoxic quinoline alkaloid that inhibits topoisomerase I, which results in prevention of DNA unwinding and consequent cell death [4, 5]. Although CPT showed remarkable therapeutic potential in preliminary clinical trials, the drug subsequently failed due to toxicity, poor bioavailability, poor solubility in biological fluids, inappropriate pharmacokinetics, and lack of efficacy within a tolerable dose range [5].

We hypothesized that sodium-R-alpha lipoate (Na-RALA) is a selective, non-cytotoxic agent ideal for use in combination therapy with CPT. Na-RALA is the sodium salt of the R-enantiomer of alpha lipoic acid (ALA). ALA is an organo-sulfur compound that serves as an essential metabolic cofactor for several enzyme complexes. We hypothesized that ALA may be an ideal agent for combination therapy of NSCLC for several reasons, including, 1) it has shown in vitro and in vivo evidence of anticancer activity [6-9]; 2) it has already been used clinically in a number of conditions and has shown a lack of toxicity at fairly high doses [10], 3) it has shown selective cytotoxic effects against cancer cells (i.e., no effect on “normal” cell viability) [9], 4) it has favorable pharmacokinetic parameters (e.g., water solubility and high bioavailability) [11], and 5) it has potent antioxidant and anti-inflammatory activities, which may exert a

chemoprotective effect on normal tissues during toxic chemotherapy [12]. In addition, the sodium salt of the R-(+) enantiomer of ALA was selected for the following reasons, 1) only the R-(+) enantiomer is endogenously synthesized and obtained through the diet, 2) the R-(+) enantiomer is more pharmacologically active and metabolically potent both in vitro and in vivo [13-15], and 3) Na-RALA is likely to be more advantageous than other forms of ALA in terms of in vivo application due to greater water solubility and a much more favorable pharmacokinetic profile [11].

The major objective of this thesis is to conduct a comprehensive in vitro and in vivo evaluation of the effects of CPT, Na-RALA, and combinations thereof on NSCLC. More specifically, the major aims are: 1) Evaluate the interactive cytotoxic effects of CPT, Na-RALA, and combinations thereof on A549 human NSCLC cells and determine optimal concentration ranges for in vivo evaluation; 2) Evaluate the effect of CPT, Na-RALA, and combinations thereof on in vitro hallmarks of cancer, namely migration, invasion, senescence, and angiogenesis,; and 3) Evaluate the effects of CPT, Na-RALA, and combinations thereof in vivo on an orthotopic NSCLC mouse model.

2. BACKGROUND AND SIGNIFICANCE

2.1 The Lung

The lungs are sponge-like organs that are part of the respiratory system. During breathing, air enters the mouth or nasal passage and travels down the windpipe or trachea. The trachea splits into two sets of tubes, the bronchial tubes, which lead to the left and right lung. The bronchi branch off into smaller and smaller tubes that eventually end in small balloon-like sacs called alveoli. The alveoli are where oxygen, carbon dioxide, and other substances are exchanged between the lungs and the blood stream.

The lungs are divided into sections, called lobes. The right lung has three lobes and the left has two lobes. The lungs contain many different types of cells. Most cells in the lung are epithelial cells. Epithelial cells line the airways and produce mucus, which lubricates and protects the lung. The lung also contains nerve cells, hormone-producing cells, blood cells, and structural or supporting cells.

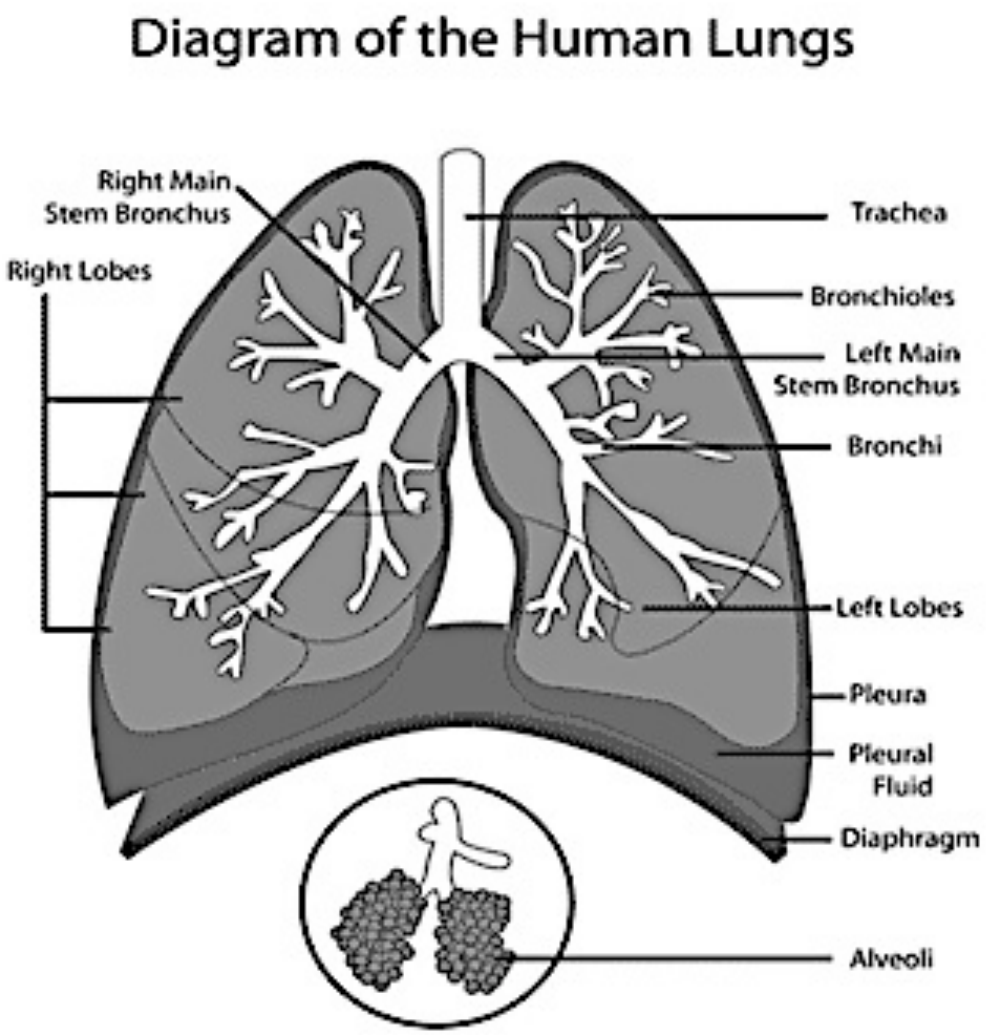

FIGURE 1 Diagram of the Human Lungs

2.2 LUNG CANCER

Lung cancer is the leading cause of cancer deaths in the United States and worldwide [1, 2, 16]. As one of the most important, prevalent, and deadly diseases in respiratory medicine, lung cancer represents a heterogeneous group of disorders unified by the growth and possible metastasis of solid tumors originating in the tissues of the lungs. Lung cancer mainly develops from pulmonary parenchymal or bronchial supportive tissues. Lung cancer also represents the most preventable respiratory disease in the world and, while its incidence is decreasing in the US and the developed world (mostly due to a decrease in the prevalence of smoking), it's classified as an outright epidemic in developing countries. According to World Health Organization (WHO) [1], the prevalence of lung cancer is ranked 1st in men and 4th in women, with approximately 1.7 million new cases diagnosed every year worldwide. The estimated number of cases in the US, where 15% of all diagnosed cancers are lung cancer, was 226,160 in 2012. Lung cancer is also the leading cause of cancer deaths and preventable deaths in men and women in both the United States and the world as a whole, surpassing prostate, breast, and colorectal cancers combined. According to World Health Organization fact sheet N°297 published in February 2011, lung cancer killed 1.4 million people in 2008. The estimated number of deaths in the US in 2012 was 160,340. It is estimated that approximately $10.3 billion per year is spent in the United States on lung cancer treatment alone [1, 2, 16].

New Cases		Deaths	
Prostate	241,740	Lung	160,340
Breast	229,060	Colorectal	51,690
Lung	226,160	Breast	39,920
Colorectal	143,460	Prostate	28,170

Table 1 Number of Cancer Cases and Deaths in the United States, 2012

The most important breakthrough in the epidemiology of lung cancer since the disease started to increase in incidence throughout the early-mid 1900s was the 1950 landmark article by Sir Richard Doll and Austin Hill which confirmed suspicions that lung cancer was associated with smoking [17]. It is now known that the most common cause of lung cancer is long-term tobacco smoking, accounting for 85% of all lung cancer cases [2, 18]. It is worth noting that he lag time between when a person starts smoking and when cancer develops can be 30 years. Non-smokers account for 15% of lung cancer cases, and these cases are attributed to genetic factors and exposure to radon gas, asbestos, air pollution, and second-hand smoke.

Lung cancer is generally divided into two main categories: non-small-cell lung cancer (NSCLC) and small cell lung cancer (SCLC). This is a histological classification based on the size and appearance of the comprising cells. In SCLC, the cells appear small and round. NSCLC, by definition, is any type of epithelial lung cancer other than SCLC. NSCLCs are also grouped together because of the similarity in treatment. NSCLC accounts for the majority of lung cancer cases (85-90%). While there is only one currently recognized subtype of SCLC, there are several subtypes of NSCLC [2].

Lung cancer is most often an insidious disease, producing subtle or no symptoms in early-stage disease [2, 19]. In general, the most common symptoms are chest pain, shortness of breath, frequent coughing (including coughing up blood), difficulty breathing, hoarseness, difficulty swallowing, wheezing, loss of appetite, fatigue, and weight loss. Consequently, most lung cancer cases are diagnosed incidentally after a chest radiograph performed for other reasons. In fact, in approximately 25% of all cases, individuals diagnosed with lung cancer showed no signs or symptoms whatsoever. There

is evidence that most patients are diagnosed based on clinical examinations and radiological investigations alone, without histological evidence. In a majority of these cases, the disease had already reached an advanced stage, resulting in a generally poor prognosis [2]. The overall survival rate five and ten years after diagnosis is 15% and 5%, respectively. It should be noted that the five-year survival rate is markedly lower than many other leading cancer sites, such as colon (65%), breast (90%), and prostate (99%).

The treatment of lung cancer primarily involves surgery (the only potentially curative treatment) [20], chemotherapy[21], radiotherapy, targeted/biological therapy [22], and combinations thereof. The distinction between NSCLC and SCLC is important in this regard as NSCLC is sometimes treated with surgery, whereas SCLC usually responds better to chemotherapy and radiation. Despite advances in technology that have allowed earlier diagnoses and advances in the above treatment options, the low survival rates post-diagnosis of lung cancer cases necessitates a focus on skilled palliative care.

2.3 NON-SMALL CELL LUNG CANCER

As stated earlier, lung cancer is histologically classified into two main types. NSCLC is by far the most prevalent type of lung cancer, accounting for approximately 85-90% of all lung cancer cases [2]. NSCLC is further classified into three major histologic subtypes that account for approximately 90% of all cases: adenocarcinoma, squamous-cell lung carcinoma, and large cell lung cancer. Other less common types of NSCLC which account for approximately 10% of cases are: pleiomorphic NSCLC, carcinoid tumor, and salivary gland carcinoma. In addition, it should be noted that all types of NSCLC occur in unusual histologic variants [2].

Adenocarcinoma, which accounts for approximately 40% of lung cancers, is the most prevalent sub-type of NSCLC and arises from the bronchial mucosal glands. It is the most common type of lung cancer among nonsmokers [2].

Squamous cell lung carcinoma, also called epidermoid carcinoma, arises in the squamous cells of the lung and is nearly always caused by smoking. Squamous cells are formed from so-called *reserve cells. Reserve cells* are round cells that replace injured or damaged cells in the epithelium of the bronchi. Tumors formed from squamous cells are usually found in the center of the lung, either in a major lobe or in one of the main airway branches. They may grow to large sizes and form cavities in the lungs [2].

Large cell carcinoma, also called undifferentiated lung cancer, is poorly differentiated and the diagnosis of exclusion in NSCLC. Large cell carcinoma accounts for 10-15% of lung cancers, typically manifesting as a large peripheral mass on chest radiograph. It appears to be decreasing in incidence because of improved diagnostic techniques. Histologically, this type has sheets of highly atypical cells with focal necrosis, with no evidence of keratinization (typical of sqaumous cell lung carcinoma) or gland formation (typical of adenocarcinomas) [2].

2.3.1 EPIDEMIOLOGY

UNITED STATES STATISTICS

In the United States, lung cancer incidence is the second only to breast cancer in women, and it is second only to prostate cancer in men. However, it is the leading cancer killer in both sexes in the United States. According to the World Cancer Research Fund's (WCRF) Expert Report, the United States is currently 8th in the world in overall (both

sexes) lung cancer rate. In 2014, approximately 224,210 lung cancer cases (15% of all cancers) will occur and approximately 159,260 deaths (30% of all cancer deaths) were expected [2, 23-25]. From 1991-2005, the incidence of lung cancer in men has decreased each year by 1.8%; however, the incidence has increased by 0.5% per year for women over that same period. Lung cancer death rates for US women are among the highest in the world, ranking at an astounding 3rd-highest rate. Although in the United States death rates among males are higher than among females (approximately double), rates for US men are still lower than rates among men in several other countries around the world, with a ranking not amongst the top 20 [2, 23-25].

These trends in US death rates run parallel to trends in smoking prevalence over the past 50 years. Overall, the prevalence of smoking is approximately 21.6% in the United States and has remained unchanged over the past 15 years [2, 23-25].

INTERNATIONAL STATISTICS OF NSCLC

Lung cancer is now the most commonly diagnosed cancer in the world, and its incidence continues to grow. In 2012, an estimated 1.4 million new cases of NSCLC were diagnosed globally, accounting for approximately 12% of the global cancer burden. An estimated 1.35 million lung cancer deaths occurred in 2007. Among all cancers, lung cancer now has the highest mortality rate in most countries, with industrialized regions such as North America and Europe having the highest rates. Several differences exist in lung cancer incidence according to geographic area. The highest incidence occurs in the Hungary and Serbia (>100 cases per 100,000 population per year). The lowest incidence rate occurs in Senegal and Nigeria (< 1 case per 100,000 population per year). With

increased smoking in developing countries, the incidence is expected to increase in the next few years, notably in China and India [2, 23, 24].

AGE DISTRIBUTION OF NSCLC

Lung cancer, and NSCLC more specifically, occurs predominately in persons aged 50-70 years. About 2 out of 3 people diagnosed with any type of lung cancer are 65 or older. The probability of developing lung cancer remains very low until age 39 years in both sexes.; fewer than 2% of all cases are found in people younger than 45. It then slowly starts to rise and peaks among those older than 70 years. The risk of developing lung cancer remains higher among men in all age groups after age 40 years [2, 23, 24].

SEX DISTRIBUTION OF NSCLC

Lung cancer is more common in men than in women, with approximately twice as many cases occurring in men than in women. In the United States, Northern Europe, and Western Europe, the prevalence of lung cancer has been decreasing in men. In Eastern and Southern European countries, the incidence of lung cancer has been rapidly increasing. Most Western countries have encountered an alarming trend of increasing prevalence in women and younger patients. Women have a higher incidence of localized disease at presentation and of adenocarcinoma and typically are younger when they present with symptoms [2, 23, 24].

In the United States, the probability of developing lung cancer remains equal in both sexes until age 39 years (0.03% or approximately 1 in 3,000). It then starts to increase among men compared with women, reaching a maximum in those older than 70

years (6.74% vs. 4.61% or 1 in 15 vs. 1 in 22, among men and women respectively) [23-25].

RACIAL DISTRIBUTION OF NSCLC

Whereas lung cancer incidence rates are similar among African American and Caucasian women, lung cancer occurrence is approximately 45% higher among African American men than among Caucasian men [2, 23, 24]. This increased incidence has been attributed to differences in smoking prevalence; however, recent evidence suggests a slight difference in susceptibility. From 1995-2001, the 5-year relative survival rate was 13% lower in African Americans compared with Caucasians. This racial gap persisted within each stage at diagnosis for both men and women[25].

Trends in 5-year survival rates in lung cancer from 1975-2003 revealed that while moderate increases occurred in 5-year survival rates among Caucasians, survival rates remained unchanged in the African American population. Current 5-year survival rates are estimated to be 16% among caucasians and 13% among non-caucasians [2, 23, 24].

2.3.2 RISK FACTORS FOR NSCLC

As previously stated, the most important breakthrough in the history of lung cancer was the discovery that smoking is a leading cause of lung cancer [17, 25]. Generally, global lung cancer trends have followed the trends in smoking, with a lag time of several decades [18, 26]. The U.S. Surgeon General estimates that approximately 90% of lung cancer deaths in men and 80% of those in women are caused by smoking. Lung cancer incidence has been declining in several countries, including the United States, Canada, the United Kingdom, and Australia, predominately due to a decrease in the

prevalence of smoking. Lung cancer incidence among women, however, continues to increase in several parts of the globe, although it has begun to plateau in the United States. Notably, despite a very low rate of smoking, Chinese females have a higher incidence of lung cancer than European females.

Men and women who smoke are 23 and 13 times, respectively, more likely to develop lung cancer. Nonsmokers have a 20% to 30% greater chance of developing lung cancer if they are exposed to secondhand smoke at home or at work. Environmental and occupations exposure to secondhand smoke causes approximately 3,400 lung cancer deaths among nonsmokers each year.

In addition to smoking, environmental and occupations exposure to second-hand smoke, radon, arsenic, asbestos, chromates, chloromethyl ethers, nickel, polycyclic aromatic hydrocarbons, radon progeny, other agents, air pollution, and radiation therapy to the breast or chest are other risk factors for the development of lung cancer. Of these, exposure to radon gas from soil and building materials is estimated to be the second leading cause of lung cancer in the United States and Europe [25].

Genetic mutations that cause lung cancer, and cancer in general, occur in two types of genes: tumor-suppressor genes (anti-oncogenes), which prevent cells from endlessly proliferating and promote apoptosis, and proto-oncogenes, which promote the proliferation of cells and cause defects in the conduction of apoptosis (when a proto-oncogene is mutated, it is then called an oncogene).

Various causes lead to mutations in either type of gene and start the cascade of tumor growth. It is unlikely that a single specific genetic mutation causes all lung cancers. It takes a variety of mutations to cause lung cancer. The Lung Cancer Mutation

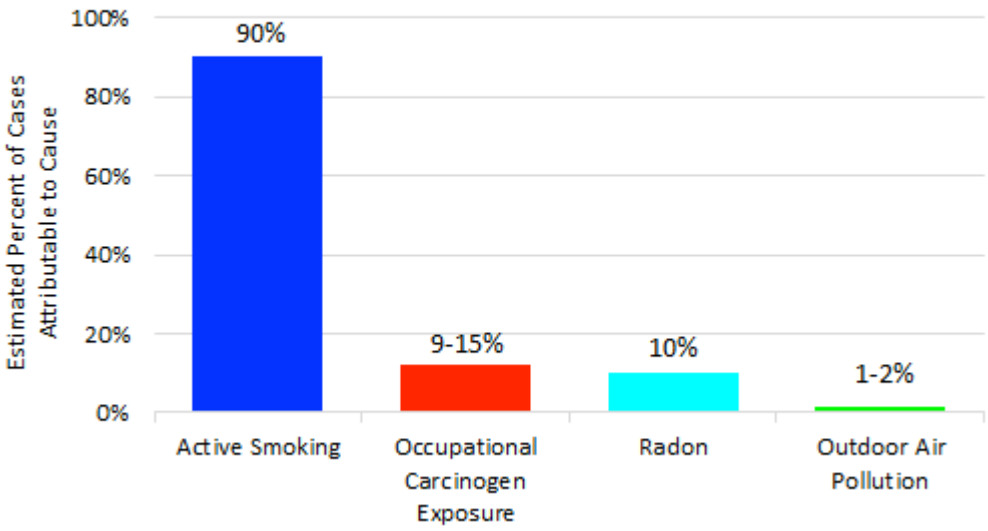

FIGURE 2 Estimated Attributable Portion of Lung Cancer Cases by Cause

Consortium (LCMC) represents the largest national initiative to prospectively examine NSCLC tumors, and match patients to the best possible therapies. Currently, the LCMC includes 16 leading cancer centers across the country. The following mutations are among those under investigation [27-29]:

EGFR mutations: EGFR (epidermal growth factor receptor gene) is a family of genes that can mutate and promote tumor growth. This gene mutation is often implicated in non-smokers. Activation of the epidermal growth factor receptor (EGFR) protein stimulates protein tyrosine kinase, which leads to activation of signaling pathways associated with cell growth and survival. HER2 is a related gene under study that plays a role in regulating cell growth.

KRAS muations: The chemical BPDE (benzo(a)pyrene diol epoxide), a byproduct of tobacco smoke, is implicated in a number of genetic mutations, including those to an oncogene called *K-ras* and to three tumor-suppressor genes known as *p53*, *PPP2R1B*, and *p16*. (Tumors that contain the p53 mutation are generally more resistant to chemotherapy).

Rb mutations: Another important contributor to lung cancer is a genetically defective protein called retinoblastoma (*Rb*), which is associated with very aggressive tumors. Low levels of the normal Rb gene may sometimes predict aggressive cancer, especially in patients with small cell lung cancer.

Abnormalities in the FHIT gene: FHIT (fragile histidine triad) is a tumor suppressor gene. The inactivation of this gene is an early event in different types. In

NSCLC, inactivation of the FHIT gene causes the epithelial cells lining the lung to become more vulnerable to the effects of tobacco smoke and other carcinogens.

Alpha1-antitrypsin mutations: Alpha1-antitrypsin is an enzyme that normally protects the walls of the alveoli in the lungs. People who carry a common variation in the gene for alpha1-antitrypsin are 70% more likely to develop lung cancer than those without the mutation, regardless of whether they are smokers or non-smokers.

ALK mutations: ALK (anaplastic lymphoma kinase) is a tyrosine kinase that rearrangements of which were reported in NSCLC in 2007. It was later shown that the EML4-ALK fusion gene is responsible for approximately 3-5% of NSCLC cases.

Many other gene mutations have been implicated in lung cancer including BRCA1, RAP80, RRM1, ERCC1, and TS. Current research continues to explore the complex relationship between various genes that play a role in cell proliferation and what environmental factors give rise to cancer [27-29]. Medical centers are beginning to test lung tumors for specific gene mutations affecting tumor growth. The hope is that an accurate "genetic fingerprint" can help physicians prescribe the most effective and appropriate treatment options [27-29].

Gene	Alteration	Frequency in NSCLC
AKT1	Mutation	1%
ALK	Rearrangement	3–7%
BRAF	Mutation	1–3%
DDR2	Mutation	~4%
EGFR	Mutation	10–35%
FGFR1	Amplification	20%
HER2	Mutation	2–4%
KRAS	Mutation	15–25%
MEK1	Mutation	1%
MET[a]	Amplification	2–4%
NRAS	Mutation	1%
PIK3CA	Mutation	1–3%
PTEN	Mutation	4–8%
RET	Rearrangement	1%
ROS1 [a]	Rearrangement	1%

Table 2 Some Common Mutations in NSCLC

2.3.3 STAGING AND PROGNOSIS

All cancers are staged to define the extent or severity to which the cancer has developed. Staging describes the severity of a patient's cancer based on the extent of the primary tumor and whether or not cancer has metastasized. Staging is important for several reasons, including helping the treating physician choose an appropriate treatment plan, determining a patient's general prognosis, and in providing data and information for research purposes and clinical trial suitability and evaluation.

Staging systems for cancer are defined by common clinical and pathological elements of the disease:

1) site of the primary tumor; 2) tumor size and number of tumors; 3) lymph node involvement; 4) cell type and tumor grade; 5) the presence or absence of metastases.

As in other types of cancer, in NSCLC, the determination of stage is important in terms of the therapeutic and prognostic aspects of the disease. A careful initial diagnostic evaluation defining the location and determining the extent of primary and metastatic tumor involvement is critical for the appropriate care and treatment of patients. The information and procedures used to determine staging in NSCLC include the following: history, physical examination, routine laboratory examination, chest x-ray, chest CT scan with infusion of contrast material, and fluorodeoxyglucose-positron emission tomography (FDG-PET) scanning.

NSCLC is staged according to the following criteria:

Stage IA- the tumor is less than 3 cm, isn't in a main bronchus, and hasn't spread to any lymph nodes

Stage IB - the tumor doesn't invade any organs, isn't too close to the trachea if it is in the main bronchus, doesn't cause obstruction of the lung, and hasn't spread to any lymph nodes

Stage IIA- the tumor is less than 3 cm, isn't in a main bronchus and has spread to lymph nodes on the same side as the tumor

Stage IIB - the tumor doesn't invade any organs, isn't too close to the trachea if it is in the main bronchus, doesn't cause obstruction of the entire lung but has spread to hilar lymph nodes (lymph nodes in the outer regions of the lung) on the same side as the tumor.

Stage IIIA - the tumor can have spread to different types of lymph nodes than Stage II (called mediastinal or subcarinal), but they are still on the same side as the tumor and it hasn't invaded any vital organs

Stage IIIB - the tumor has either invaded vital adjacent organs and/or spread to lymph nodes on the other side of the mediastinum as the tumor, or specific lymph nodes called scalenes or supraclavicular. Also, the patient may have tumor spread to the fluid surrounding the lung

Stage IV- the tumor has spread (metastasized) to other organs in the body outside the lungs (like the bones, brain or liver).

NSCLC Stages and Survival Rates		
Stage	Frequency of Diagnosis	Five-Year Survival (%)
I	10%	>60%
II	20%	30%–50%
IIIA	15%	15%–30%
IIIB	15%	3%–6%
IV	40%	<1%

Table 3 NSCLC Stages and Survival Rates

2.3.4 TREATMENT

As stated earlier, lung cancer remains the most common diagnosed and deadliest cancer in the world [1, 2]. Current treatment options for NSCLC include surgery [30, 31], chemotherapy [21, 32, 33], targeted/biological therapy [22, 28], radiotherapy, and combinations thereof. Surgery, along with chemotherapy, continues to be the mainstay of treatment for early-stage and localized disease [30, 31]. Chemotherapy is generally indicated for patients with advanced NSCLC and also benefits patients with earlier stages of the disease. Targeted/biological therapy is a significant advance in the molecular-based treatment of NSCLC that has made its way into the clinic in cases where cytotoxic chemotherapy has plateaued [22, 28, 33]. Patients with potentially resectable tumors with medical contraindications to surgery or those with inoperable stage I disease and with sufficient pulmonary reserve may be candidates for radiation therapy. Multimodal therapy, therapy that combines more than one method of treatment, has become the norm for regionally advanced disease [2].

Surgery is the only potentially curative treatment for early-stage and localized NSCLC. In NSCLC, surgery is often employed in cancers up to and including stage IIIA [30, 31, 34]. The purpose of the surgery is to remove all of the cancer if possible. If the tumor is small and in a favorable location, or the patient has limited lung function, the surgeon may choose to remove the tumor with a small section of lung; this is called a wedge resection. Most times the surgeon will choose to remove the entire lobe of the involved lung; this is known as a lobectomy. In certain circumstances, the surgeon may have to remove the entire lung affected by the cancer; and this is known a pneumonectomy. It should be noted that not every patient can tolerate these types of

surgery. Patients with diminished lung function due to other diseases may not be able to survive after such a surgery, or they may be severely limited in their activities. Preoperative pulmonary function tests (PFT's) are used to help predict who is a good candidate for surgery. Sometimes, a quantified ventilation perfusion scan is prescribed to show the amount of lung tissue in each area that is functional. These tests may help the surgeon to predict how much lung function will be lost based on the amount of lung that will need to be removed, and how well the patient will feel after surgery [30, 31, 34].

As a class, NSCLC is relatively insensitive to chemotherapy compared with SCLC. For some time, the treatment of NSCLC with cytotoxic chemotherapy remained controversial, given the unclear impact on patient survival [2]. The first piec of evidence that chemotherapy produced a significant survival benefit in patients with advanced NSCLC came in 1995 when a meta-analysis showed that platinum-based chemotherapy conferred a 2-month improvement in median survival over best supportive care [21]. The consensus now is that chemotherapy is generally indicated for patients with advanced NSCLC because the results of many large randomized phase III clinical trials have established that modern chemotherapies offer superior survival and symptom alleviation than best supportive care [2, 26, 33]. More specifically, platinum agents have currently shown the greatest promise in patients with NSCLC, and as such, have been the worldwide standard based on meta-analyses suggesting superiority over non-platinum-based therapy [33]. In general, these agents induce their cytotoxic effects by targeting cellular DNA. Recent reviews of chemotherapy for NSCLC identified the most frequently used active agents as cisplatin (Platinol®), carboplatin (Paraplatin®), paclitaxel (Taxol®), albumin-bound paclitaxel (Abraxane®), docetaxel (Taxotere®),

gemcitabine (Gemzar®), vinorelbine (Navelbine®), Irinotecan (Camptostar®), etoposide, vinblastine, and, pemetrexed (Alimta®). Response rates to single agents are approximately 20%. It is now accepted that two-agent combination therapy (doublet) is better than monotherapy because it provides an overall survival benefit [33]. However, no platinum-based doublet regimen has been proven superior to another on the end point of overall survival in clinical trials. Adding a third agent (triplet) may increase the response rate in advanced NSCLC, but does not improve overall survival. The only exception thus far is the inclusion of a third agent in the category of targeted/biological agents [22, 35]. Overall, the current first line standard of care with chemotherapy-based regimens for advanced NSCLC demonstrates a response rate of about 24-30%, with a median survival of 10.3 to 12.3 months and a progression free survival of 4.8 to 5.1 months.

Selection of chemotherapy also is based on the specific type of NSCLC. In general, different drugs are recommended for adenocarcinoma and squamous cell carcinoma, although most regimens help with both. Also, treatments that are used for adenocarcinoma are the most effective in treatment for large cell carcinoma. Treatment usually is given for four to six cycles if there is tumor response or stable disease. In non-squamous NSCLC, options include: 1) Cisplatin-based doublet with or without targeted therapy [22]; 2) Carboplatin/paclitaxel [33]. In squamous NSCLC, a platinum double is the most common chemotherapeutic regimen[33].

A discussion of chemotherapy in the treatment of NSCLC is not complete without a mention of toxicity. Although multi-drug combinations have repeatedly shown superior efficacy, it comes at the expense of added toxicity. Side effects of chemotherapy

include anemia, neutropenia, thrombocytopenia, nausea, vomiting, diarrhea, constipation, mucositis, peripheral neuropathy, alopecia, infection, pain, and fatigue. Patients may experience changes in appetite, skin, nails, vision, or hearing. The patient also may feel flu-like symptoms, including body and muscle aches and pain, fever, chills, headache, and nasal congestion.

As mentioned earlier, an exciting advance in the treatment of NSCLC is targeted/biological therapy [22]. Chemotherapeutic drugs are effective because they exert a cytotoxic effect on cancer cells that proliferate rapidly. However, many normal cells also proliferate rapidly, such as cells of the digestive tract, hair follicles, and blood. When normal cells are exposed to cytotoxic chemotherapeutic drugs, many undesirable side effects may occur. Targeted/biological therapies address this issue by interfering with specific molecular aspects of cancer cells, giving rise to more specificity and an avoidance of damage to normal cells. Targeted therapy [22] consists of either monoclonal antibodies (names ending in "-ab") that target cancer cell membranes or small molecules (names ending in "-ib") that work directly intracellularly. Over the past decade, a multitude of targeted agents have been explored in the treatment of advanced NSCLC [22]. Thus far, two broad classes of agents have made their way into the clinic: (1) vascular endothelial growth factor (VEGF)-directed therapies and (2) antagonists of the epidermal growth factor receptor (EGFR). In the former category, the monoclonal antibody bevacizumab (Avastin®) has shown landmark improvements in survival when added to cytotoxic therapy [3]. Small molecule tyrosine kinase inhibitors (TKIs) targeting the VEGF receptor (i.e., sunitinib, sorafenib, and vandetanib) showed activity in

phase II clinical studies. With respect to EGFR-directed therapies, the TKIs gefitinib and erlotinib have demonstrated significant benefit, and have uncovered valuable information regarding the biology of lung cancer. Outside of therapies directed specifically at VEGF- and EGFR-mediated signaling, Pemetrexed (Alimta®) is an antifolate drug that blocks multiple pathways in folate metabolism [36]. Also, trials evaluating insulin-like growth factor-1 receptor (IGF-IR)-targeting agents, cyclooxygenase-2 (COX-2) inhibitors, c-met inhibitors, irreversible pan-HER inhibitors, mammalian target of rapamycin (mTOR) inhibitors, and histone deacetylase (HDAC) inhibitors are ongoing. Inhibitors of ALK show great promise in patients with the relevant gene translocation (EML4-ALK fusion gene)[22]. Maintenance chemotherapy, the ongoing administration (beyond four to six cycles) of at least one chemotherapeutic agent given during primary treatment, almost always incorporates targeted/biological agents and is sometimes given to extend long-term benefit from treatment. Common examples of maintenance chemotherapy in NSCIC are: bevacizumab continued after four to six cycles of cisplatin-doublet and bevacizumab, and pemetrexed, continued after four to six cycles of cisplatin and pemetrexed for patients with non-squamous cell NSCLC.

Radiation therapy uses high-energy rays (such as x-rays) or particles to kill cancer cells. There are 2 main types of radiation therapy – external beam radiation therapy and brachytherapy (internal radiation therapy). Primary radiotherapy (with curative intent) can be considered in patients with inoperable stages I or II of the disease and sufficient pulmonary reserve. Analysis of one randomised and 26 nonrandomised studies in more than 2000 patients receiving radical radiotherapy for stage I or II disease found that 5-year survival rates ranged from 0 to 42%. Primary radiotherapy used to be the ‘gold

standard' treatment in locally advanced NSCLC. Patients with potentially resectable tumors with medical contraindications to surgery or those with inoperable stage I disease and with sufficient pulmonary reserve may be candidates for radiation therapy with curative intent. Primary radiation therapy often consists of approximately 60 Gy delivered with megavoltage equipment to the midplane of the known tumor volume using conventional fractionation. A boost to the cone down field of the primary tumor is frequently used to enhance local control. Careful treatment planning with precise definition of target volume and avoidance of critical normal structures to the extent possible is needed for optimal results; this requires the use of a simulator.

Multimodal therapy combines any of the above treatment options with the goal of improving or maintaining therapeutic outcome. Multimodal therapy is the norm for advanced cases of NSCLC. Common examples of multimodal treatment plans are:

Stage I NSCLC

- Surgery (radiation if not a surgical candidate) with or without chemotherapy
- A clinical trial of chemotherapy or radiation therapy following surgery.
- A clinical trial of surgery followed by chemoprevention.

Stage II NSCLC

- Chemotherapy followed by surgery (radiation if not a surgical candidate).
- Surgery (radiation if not a surgical candidate) followed by chemotherapy.

- A clinical trial of radiation therapy following surgery.

Stage IIIA NSCLC

- Surgery followed by chemotherapy.
- Chemotherapy followed by surgery.
- Surgery followed by chemotherapy combined with radiation therapy.
- Surgery followed by radiation therapy.
- Chemotherapy and radiation therapy given as separate treatments over the same period of time.

Stage IIIB NSCLC

- Chemotherapy followed by external radiation therapy.
- Chemotherapy and radiation therapy given as separate treatments over the same period of time.
- Chemotherapy followed by surgery.

Stage IV NSCLC

- Maintenance therapy after combination chemotherapy.
- Combination chemotherapy and targeted/biological therapy with a monoclonal antibody.

2.3.5 PREVENTION

The best way to prevent lung cancer is the avoidance or cessation of smoking (all forms, including pipes, cigars, and marijuana). In addition, avoidance or an effort to minimize exposure to second-hand smoke will decrease the risk of lung cancer. People living in areas with high levels of radon should sure ensure adequate ventilation. Detectors can be used to ensure that radon levels are low. People working in an industries where there is high exposure to substances known to cause lung cancer should make sure to use all the proper protective equipment and attire available.

Although not yet confirmed, there has been some suggestion that a diet high in fruits and vegetables may decrease the risk of lung cancer. Many compounds, including antioxidants like vitamin A, vitamin E, and beta-carotene, have been suggested to decrease the risk of lung cancer. None of these has been shown to be beneficial in randomized controlled trials and therefore cannot be recommended for this purpose. In fact, large clinical trials have shown an increased risk of lung cancer in patients with an increased intake of vitamin E, vitamin A, and beta-carotene.

Chemoprevention studies have shown some promise as a strategy to decrease the incidence of lung cancer [37]. Inositol (cyclohexane-1,2,3,4,5,6-hexol) is currently being investigated as a chemopreventive compound that may prevent the development of lung cancer in current or former smokers who have precancerous lesions in their lungs [37]. It also is being studied in patients who had a stage I or II NSCLC that was completely removed with surgery. It is an endogenous compound mainly synthesized in the kidneys and has many functions within the body.

The most recent promising results of lung cancer chemoprevention come from the University of Colorado, where investigators showed that iloprost (Ventavis®), a drug used to treat pulmonary arterial hypertension, scleroderma, Raynaud's phenomenon and other diseases in which the blood vessels are constricted and blood can't flow to the tissues, improves endobronchial histology in former smokers when administered orally [38]. Further studies will determine if iloprost can in fact prevent the development of lung cancer.

The future of NSCLC prevention will rely on a sophisticated analysis of patients' genes and molecular markers for NSCLC risk. In addition, "smart drug" design and novel diagnostic techniques may decrease the risk of developing NSCLC, allowing earlier diagnoses and improving therapeutic outcome.

2.4 FUTURE PERSPECTIVES

As stated earlier, one of the distinguishing features of NSCLC is its presentation with very vague symptoms [2, 19]. Consequently, the disease is often diagnosed in advanced stages where surgery can no longer offer a curative outcome. For this reason, chemotherapy remains the workhorse of treatment regimens. However, the success of chemotherapy is modest at best (20-30% response rate) and toxicity due to treatment remains a significant issue. In addition, multi-drug combinations consisting solely of cytotoxic chemotherapeutic agents exacerbate toxicity. A currently used alternative thus far is the addition of targeted/biological agents to cytotoxic chemotherapy, as discussed earlier. For example, a randomized, phase II trial demonstrated improvement in response

rate (response rate; 31.5% *vs.* 18%) and median overall survival (17.7 *vs.* 14.9 months) with the addition of bevacizumab to carboplatin and paclitaxel chemotherapy [3]. On October 11, 2006, the U.S. Food and Drug Administration granted approval for bevacizumab, administered in combination with carboplatin and paclitaxel, for the initial treatment of patients with unresectable, locally advanced, recurrent, or metastatic, non-squamous NSCLC. Approval is based on a significant improvement in overall survival [35]. Similarly, Ipilimumab, which is an anti-cytotoxic T-cell lymphocyte-4 monoclonal antibody, moderately improved overall survival and progression-free survival in chemotherapy-naïve NSCLC patients [39].

Another developing option in the treatment of NSCLC is personalized medicine. Pathology will be key in supporting this approach to treatment decision-making. Pathologists are attempting to perform the most complete and accurate histological subtyping of lung tumors possible, supported by predictive immunohistochemistry and the assessment of relevant biomarkers. The mutations listed earlier in this discussion will be among the many targets that can be exploited to increase therapeutic response without a concomitant increase in drug-related toxicity. Sirolimus (rapamycin, Rapamune®) is an oral rapalogue which has demonstrated synergism in combination with pemetrexed in vitro and in vivo in NSCLC models. PI3K inhibition, Akt inhibition, and EGFR inhibition are other examples of targeted/biological agents that can be combined with cytotoxic chemotherapy to increase therapeutic response in selective patients while decreasing toxicity as seen in patients treated only with cytotoxic agents [36]. Despite enthusiasm for the use of molecular testing and molecularly targeted/biological agents in patients with advanced NSCLC, some patients are not candidates for upfront treatment

with molecular agents. Chemotherapy therefore remains the workhorse of treatment for patients with advanced NSCLC.

Another less commonly mentioned option is chemosensitization. Chemosensitization is the use of agents or other strategies to sensitize tumors to the effects of chemotherapy. There are countless examples of strategies that fall under the category of chemosenstization. In fact, the concomitant use of radiotherapy and/or targeted/biological therapy [40] with chemotherapy, or the use of more than one chemotherapeutic agent, were at first coined as chemosensitization strategies. Since then, a variety of strategies have been investigated, including immunomodulation[41], phytochemicals [42-44], small interfering RNA (siRNA) [45], cyclotides [46], and signal transduction modulation with miscellaneous pharmacological agents [47, 48], and metabolic agents [49-52].

3. SPECIFIC AIMS

Lung cancer is the most common cause of cancer-related mortality among both men and women in the United States and worldwide, killing more people than breast, prostate, and colon cancers combined. It is estimated that 1.37 million people worldwide die of the disease annually. NSCLC accounts for the majority of lung cancer cases worldwide and thus remains a primary focus of therapeutic lung cancer research.

Most patients are diagnosed at late stages of NSCLC and are therefore treated with cytotoxic chemotherapy. However, efficacy is modest at best and treatment-related toxicity remains a significant drawback. Novel approaches to improve upon NSCLC chemotherapeutic regimens are needed. I hypothesized that a combination of CPT and Na-RALA may offer comparable, if not better, efficacy and lower toxicity than current chemotherapeutic regimens. The hypothesis is based on the fact that NSCLC, among many cancers, displays metabolic abnormalities that can be exploited as a targeting mechanism. The objective of this thesis is initiate a comprehensive in vitro and in vivo evaluation of the effects of CPT and Na-RALA on NSCLC. The results will be realized through the following specific aims:

Specific Aim 1: Evaluate the interactive cytotoxic effect of CPT, Na-RALA, and combinations thereof on A549 human NSCLC cells and determine optimal concentration ranges for in vivo evaluation.

Hypothesis: A combination of CPT and Na-RALA will display synergy in cytotoxicity induction in A549 NSCLC cells and will display lower toxicity/higher selectivity compared to CPT alone.

Specific Aim 2: Evaluate the effects of CPT, Na-RALA, and combinations thereof on in vitro hallmarks of cancer, namely migration, invasion, senescence, and angiogenesis.

Hypothesis: A combination of CPT and Na-RALA will have potent effects on the in vitro hallmarks of cancer, and the combination will be more efficacious than CPT alone

Specific Aim 3: Develop a orthotopic xenograft mouse model of NSCLC for preliminary in vivo evaluation of the CPT/Na-RALA combination.

Hypothesis: The model displaying primary tumor onset and maetatstis incidence in the framework of time and practicality will be used for the preliminary evaluation of the CPT/Na-RALA combination.

4. SPECIFIC AIM 1

Specific Aim 1: Evaluate the interactive cytotoxic effect of CPT, Na-RALA, and combinations thereof on A549 human NSCLC cells and determine optimal concentration ranges for in vivo evaluation.

Hypothesis: A combination of CPT and Na-RALA will display synergy in cytotoxicity induction in A549 NSCLC cells and will display lower toxicity/higher selectivity compared to CPT alone.

4.1 INTRODUCTION

Lung cancer is the most common cause of cancer-related deaths among both men and women in the United States and worldwide. Lung cancer is also among the three most common cancers in both men and women in the United States [1, 53]. Non-small cell lung cancer (NSCLC) is by far the most prevalent type of lung cancer, accounting for nearly 85% of all lung 40 cancer cases [54]. With a 5-yr survival rate of ~15% in the United States and ~8% in Europe and the developing world, NSCLC remains a highly lethal cancer despite current therapeutic options [1, 54]. Thus, there remains a critical need for more effective therapies. Early-stage NSCLC presents with vague and variable 45 symptoms [19]. For this reason, the majority of NSCLC cases are diagnosed at an advanced stage, during which surgical therapy can no longer offer a curative outcome and chemotherapy becomes a mainstay of therapy. Thus, improvement of current chemotherapeutic regimens is highly sought after. One such approach, combination therapy, has the goal of enhancing or replacing the desired cytotoxic effect of a

chemotherapeutic agent with another agent, allowing for an overall reduction in the chemotherapeutic drug and/or delivery system load. Theoretically, the use of benign agents that are selective for malignant cells (i.e., benign toward normal tissues) may not only enhance or replace the effects of chemotherapy and lower drug/delivery system load but may also impart the additional benefit of greatly reducing the potential for toxic side effects. In addition, agents with antioxidant and/or anti-inflammatory activities may exert a chemoprotective effect on normal tissues against the toxic insults of chemotherapy.

We hypothesized that one agent that fulfills these criteria is Na-RALA, the sodium salt of the R-enantiomer of alpha lipoic acid (ALA). ALA is an organosulfur compound that serves as an essential metabolic cofactor for several enzyme complexes, including pyruvate dehydrogenase complex, 2-oxoglutarate dehydrogenase complex, branched chain oxoacid complex, and acetoin dehydrogenase complex [10, 55]. ALA, whose R-enantiomer (R-alpha lipoic acid) is endogenously synthesized and obtained through the diet, has been shown to have several beneficial effects in addition to its essential metabolic function, including antioxidant, metal-chelating, anti-inflammatory, neuroprotective, wound-healing, antiaging, and hypoglycemic activities [7, 10, 55, 56]. For this reason, ALA has been used clinically in a number of conditions, including diabetic neuropathy[57], liver disease [58], and human immunodeficiency virus/acquired immunodeficiency syndrome [59]. Recently, ALA has gained considerable attention due to in vitro [6, 9, 60, 61] and in vivo [7, 62] anticancer effects. Although the exact mechanisms responsible for these effects have yet to be completely elucidated, it is most likely related to ALA's metabolic effects [9, 62]. Wenzel et al. showed that ALA induces apoptosis in the human colon cancer cell line HT-29 by increasing mitochondrial

respiration and causing a resultant increase in superoxide production [9]. In the same study, it was shown that ALA was selective for cancer cells, as it did not induce apoptosis in the normal counterpart cell line tested [9]. In addition, certain types of cancer present with a metabolic anomaly [63], hypothesized to promote cancer growth, which results in a switch from a primary reliance on oxidative phosphorylation for energy production to aerobic glycolysis, termed the Warbug Effect [63-65]. The observations that the enzyme pyuruvate dehydrogenase kinase (PDK) is involved in the expression of this metabolic switch [51] and that ALA has been shown to inhibit PDK [66], and thus potentially reverse the Warburg Effect [63], add further credence to the hypothesis that a metabolic effect is responsible for the cytotoxic effects of ALA. Interestingly, dichloroaceate, an analogue of acetic acid and an inhibitor of PDK [50], has repeatedly shown in vitro and in vivo anticancer effects both alone and when used in combination with chemotherapeutic agents such as carboplatin, cisplatin, and 5-Flurouracil [49, 50, 52]. Other potential mechanisms responsible for the anticancer effects of ALA may involve antioxidant and anti-inflammatory activities [10, 55] or inhibition of nuclear factor-kappa B (NF-κB) [56] and activator protein-1 (AP-1) [67].

The common designation “alpha lipoic acid” refers to a 50/50 racemic mixture of R- and S-alpha lipoic acid. The only reason for the presence of S-alpha lipoic acid in ALA preparations is an achiral manufacturing process. Although previously believed to be physiologically inactive, recent studies have suggested that S-alpha lipoic acid may actually compete with and inhibit the functions and effects of R-alpha lipoic acid, such as R-alpha lipoic acid’s inhibition of PDK [66], modulation of mitochondrial activity, and interaction with proteins, enzymes, and genes [11]. For these reasons, we chose the more

metabolically potent R-enantiomer [11, 13, 14] to investigate the effect of ALA on chemotherapy-induced cytotoxicity. In addition, shall Na-RALA display promising effects in vitro, this form of ALA will be far more superior in terms of in vivo application due to greater water solubility and a much more favorable pharmacokinetic profile [11].

CPT is a cytotoxic quinoline alkaloid isolated from the bark and stem of *Camptotheca Acuminata* [4, 5]. CPT's primary mechanism of action involves inhibition of topoisomerase I, which results in prevention of DNA unwinding and leads to cell death [4]. Although CPT showed remarkable therapeutic potential in preliminary clinical trials, the drug subsequently failed due to toxicity, poor oral bioavailability, poor solubility in biological fluids, inappropriate pharmacokinetics, and lack of efficacy within a tolerable dose range [4, 5]. However, topotecan, a water-soluble derivative of CPT, has previously been investigated for the treatment of NSCLC [68]. Paclitaxel is a plant alkaloid and taxane isolated from Taxus Brevifolia. Paclitaxel's mechanism of action involves a hyper-stabilization of microtubule polymers, preventing disassemblyand causing cell death. Paclitaxel (trade name Taxol®), in combination with cisplatin, is indicated for the first-line treatment of NSCLC in patients who are not candidates for curative surgery and/or radiation therapy.

CPT, paclitaxel, and analogues thereof have been used in the treatment of NSCLC, and our laboratory has extensive experience with these compounds both from a pharmacological and a drug-delivery perspective [69-73]. In particular, our laboratory has previously shown that lung targeting of a CPT pro-drug (CPT-norvaline), via passive entrapment of rigid microparticles can reduce therapeutic doses of CPT 10-fold in a rat orthotopic lung cancer model [70]. A synergy approach using Na-RALA is proposed to

further minimize the dose of CPT and reduce the dose of microparticles, thus minimizing the toxic potential of either the drug or the delivery system or both. In the current study, the cytotoxic effects of sodium-Ralpha lipoate, CPT, paclitaxel, CPT/sodiumR-alpha lipoate, and paclitaxel/Na-RALA were evaluated on A549 human NSCLC adecnocarcinoma cells. An automated computer simulation of the combinatorial effects of Na-RALA with CPT or paclitaxel was applied with CompuSyn®3.01 software to characterize the interactions (synergy, additivity, or antagonism) and determine the potential for CPT or paclitaxel dose reduction [74].

4.2 MATERIALS AND METHODS

Cell Culture

A549 human NSCLC adenocarcinoma cells (American Type Culture Collection, Rockville, MD) were cultured and passaged in Dulbecco's modified eagle medium (DMEM) supplemented with 10% fetal bovine serum (FBS) and 100 U/ml penicillin-100 µg/ml streptomycin. BEAS-2B human lung epithelial cells (ATCC) were cultured and passaged in serum-free bronchial epithelial growth medium (BEGM; Lonza Walkersville Inc.,Walkersville, MD) supplemented with 0.4% bovine pituitary extract, 0.1% hydrocortisone, 0.1% human EGF (hEGF), 0.1% epinephrine, 0.1% transferrin, 0.1% insulin, 0.1% retinoic acid, 0.1% triiodothyronine, 0.1% gentamycin amphoterecin-B (GA- 1751000), and 100 U/ml penicillin-100 µg/ml streptomycin. Both cell lines were maintained in an incubator at 37◦C with 5% CO2.

MTT Cytotoxicity Assay

CPT (Sigma Aldrich, St. Louis, MO), paclitaxel (LC Laboratories, Woburn, MA), and S-lipoic acid (Geronova Research, Carson City, NV) stock solutions were made using 100% dimethyl sulfoxide (DMSO) and Na-RALA (Geronova Research, Carson City, NV) solutions were prepared in sterile distilled water. CPT stock solutions were always made fresh to ensure stability for the duration of the studies. A549 cells were plated at a density of 1×103 cells per well in 96-well plates and cultured for 24 h, followed by treatment with the indicated compound(s) or DMSO solvent controls for CPT, paclitaxel, and S-lipoic acid treatment (0.01% to 0.1% DMSO). The concentrations used were Na-RALA 0–16 mM; CPT, 0–25 nM; paclitaxel, 0–0.06 nM; Slipoic acid, 0–10 mM; CPT/Na-RALA, 0–12 nM CPT and 0–8 mM Na-RALA; and paclitaxel/Na-RALA, 0–0.03 nM paclitaxel and 0–8 mM Na-RALA. Mixtures were made by simply mixing the working solutions used for the individual compound treatments. After 2, 4, and 6 days of incubation, 3-(4,5-methylthiazol-2-yl)-2,5-diphenyl-tetrazolium bromide (MTT; Sigma Aldrich, St. Louis, MO) was added and incubated for 2 h at 37◦ C. Formazan products were solubilized with 100% DMSO, and the optical densities were measured in a plate reader (Tecan; Mannedorf, Switzerland) at 570 nm. The effects of Na-RALA, CPT/Na-RALA, and paclitaxel/Na-RALA on BEAS-2B cell viability were investigated in the same manner.

CompuSyn®3.01 Analysis

Dose-response curves, combination indices, and dose reduction indices were generated for all treatments and time points with CompuSyn®3.01 software (Paramus, NJ) according to the manufacturer's instructions. CompuSyn®3.01 software uses an algorithm based on mass-action law (Figure 3) to simulate the interaction of 2 or more

compounds on the investigated pharmacological effect. Briefly, concentrations and corresponding effects levels (the effect of a treatment expressed as a decimal between 0 and 1, 0 being no effect and 1 being 100% effect) for all data points were input to generate a complete report of analytical results. The combination index (CI) is a parameter that indicates whether the interaction of 2 or more drugs is synergistic, additive, or antagonistic {(additive=1); synergistic (CI < 1)}; antagonistic (CI > 1)}. The CI is calculated using the following equation: {(D1/Dx1) + (D2/Dx2)} = CI, where, at a certain effect level, D1 is the dose of drug 1 when used in combination with drug 2, Dx1 is the dose of drug 1 when used alone, D2 is the dose of drug 2 when used in combination with drug 1, and Dx2 is the dose of drug 2 when used alone. The dose reduction index (DRI) is a parameter that indicates the degree to which a drug dose can be reduced when used in combination with another drug and maintain an equivalent effect level. The DRI is calculated using the following equation, Dn/Dxn = DRIn, where, at a certain effect level, Dxn is the dose of the drug required to exert the aforementioned effect level when used alone and Dn is the dose of the drug required to exert the same effect level when used in combination with another drug.

Statistical Analysis

All statistical analyses were performed with GraphPad Prism®4.0c software. Raw data for all treatments and time points was normalized and fitted with nonlinear regression using GraphPad Prism® 4.0c software (La Jolla, CA) to generate dose-response curves and calculate the half-maximal effective concentrations (EC50s) for all treatments and time points. Individual points within dose-response curves were expressed as mean ± standard error of mean. Comparisons between dose response curves within

each plot were made using the F-test. The limit for statistical significance was set at $P < 0.05$.

4.3 RESULTS

Individual Effect of CPT, Paclitaxel, Na-RALA, or S-Lipoic Acid on A549 Cells

To determine the effects of the individual compounds on A549 cells, dose-response curves were constructed for CPT, paclitaxel, Na-RALA, and S-lipoic acid after 2, 4, and 6 days of treatment (Figure 4). As hypothesized, Na-RALA (Figure 4) was found to be more potent than S-lipoic acid (Figure 4). Paclitaxel was found to be the most cytotoxic compound (Figure 4). The EC50s for CPT were 23.68, 14.76, and 7.69 nM after 2, 4, and 6 days of treatment, respectively (Table 4). The EC50s for paclitaxel were 0.0031, 0.0034, and 0.0024 nM after 2, 4, and 6 days of treatment, respectively (Table 4). The EC50s for Na-RALA when used individually in the CPT/Na-RALA arm were 3.12, 2.21, and 0.40 mM after 2, 4, and 6 days of treatment, respectively (Table 3). The EC50s for Na-RALA when used individually in the paclitaxel/Na-RALA arm were1.77, 0.70, and 0.52 mM after 2, 4, and 6 days of treatment, respectively (Table 4). The EC50s for S-lipoic acid were 3.56 and 1.54 mM after 4 and 6 days of treatment, respectively. An EC50 value for S-lipoic acid after 2 days of treatment could not calculated from the observed data.

Effect of CPT/Na-RALA and Paclitaxel/Na-RALA Combinations on A549 Cells

To determine the effects of the CPT/Na-RALA and paclitaxel/Na-RALA combinations on A549 cells, dose-response curves were constructed after treatment for 2, 4, and 6 days (Fig. 4). Figure 2 shows the CIs of the CPT/Na-RALA and

paclitaxel/sodium-Ralpha lipoate combinations at all effect levels after treatment for 2, 4, and 6 days. It was observed that the CPT/Na-RALA combination had markedly lower CIs than the paclitaxel/Na-RALA combination. The CIs for the CPT/Na-RALA combination ranged from ~0.71 to 1.5, whereas the CIs for the paclitaxel/Na-RALA ranged from ~0.8 to 9.9. The CPT/Na-RALA combination showed several CIs in the synergistic or additive range (CI ≤ 1), especially after 2 and 4 days of treatment. On the other hand, all combinations of paclitaxel and Na-RALA were antagonistic (CI > 1).

Figure 5 shows the DRIs of the CPT/Na-RALA and paclitaxel/Na-RALA combinations as a function of Na-RALA concentrations after treatment for 2, 4, and 6 days. It was found that the CPT/Na-RALA combination had markedly higher DRIs than the paclitaxel/Na-RALA combination. The DRIs for the CPT/Na-RALA combination ranged from ~2.2– to 22.6, whereas the DRIs for the paclitaxel/Na-RALA ranged from ~0.10 to 8.3. The CPT/Na-RALA combination had several DRIs greater than 10, especially after 2 days of treatment. On the other hand, almost all DRIs for the paclitaxel/Na-RALA combination were less than 5.

Effect of Na-RALA, CPT/Na-RALA, and Paclitaxel/Na-RALA on BEAS-2B Lung Epithelial Cells

To determine the effects of Na-RALA on normal BEAS-2B lung epithelial cells, dose-response curves were constructed after 2, 4, and 6 days of treatment. Concentrations of Na-RALA were the same as those used for A549 NSCLC adenocarcinoma cells. It was found that Na-RALA had no effect BEAS-2B cell viability (Figure 7). However, longer treatment times showed that Na-RALA may have exerted an anti-proliferative effect

because, although the results of the MTT assay showed lower absorbance (data not shown), examination by microscopy indicated a lack of cytotoxicity (intact, adherent colonies, as opposed to single, floating cells). To further confirm the lack of toxicity of sodiumR-alpha lipoate towards BEAS-2B cells, a "rescue experiment" was conducted in which BEAS-2B cells that had been incubated in Na-RALA were subsequently incubated in control DMEM medium. It was found that upon subsequent incubation in control DMEM medium, BEAS-2B proliferated at rates observed in normal cell culture (data not shown). Representative data shown in Figure 7 highlight the differential effect of Na-RALA on A549 NSCLC cells versus BEAS-2B "normal" lung epithelial cells.

Because the data suggested that Na-RALA is selective for A549 NSCLC cells vs. BEAS-2B "normal" lung epithelial cells, the CPT/Na-RALA and paclitaxel/Na-RALA combinations were also evaluated on BEAS-2B cells. Concentrations for the 3 compounds were as previously used. It was found that Na-RALA moderately protected BEAS-2b cells from the cytotoxic effect of CPT (Figure 8). For example, exposure to 4 nM CPT alone resulted in ~68% cell death, whereas exposure to 4 nM CPT with Na-RALA resulted in only ~10% cell death. However, Na-RALA failed to exert a chemoprotective effect on paclitaxel-induced cytotoxicity (Figure 8).

4.4 DISCUSSION

Lung cancer is among the most common and lethal cancers in the United States and worldwide. As the most prevalent type of lung cancer, NSCLC kills more people than breast, colon, and prostate cancers combined and remains one of the deadliest forms of cancer in the world. Currently used treatments for the disease include surgery,

chemotherapy, radiotherapy, biological therapy, laser therapy, photodynamic therapy, and combinations thereof. Innovative therapies targeting specific pathways associated with apoptosis, cell proliferation, and angiogenesis are also under investigation. Despite these treatment options, the general prognosis of NSCLC remains extremely poor, with a 5-year survival rate of only ~15% [2]. With chemotherapy being one of the most commonly recommended treatments in late stage disease, during which most patients are diagnosed, the search continues for more effective and less toxic chemotherapeutic strategies. One potentially viable option is combination therapy. Combination therapy can have major advantages as a chemotherapeutic strategy, including higher potency, lower toxicity, and a potential for greatly reduced therapeutic doses.

Our previous experience with CPT and paclitaxel prompted us to investigate novel, minimally toxic combination therapy for NSCLC involving the use of these agents. We hypothesized that ALA may be an ideal agent for combination therapy of NSCLC for several reasons, including, 1) it has shown in vitro and in vivo evidence of anticancer activity [62], 2) it has already been used clinically in a number of conditions and has shown a lack of toxicity at fairly high doses, 3) it has shown selective cytotoxic effects against cancer cells (i.e., no effect on "normal" cell viability), 4) it has favorable pharmacokinetic parameters (e.g., high bioavailability after oral administration) [11], and 5) it has potent antioxidant and anti-inflammatory activities, which may exert a chemoprotective effect on normal tissues during toxic chemotherapy. In addition, the sodium salt of the R-(+) enantiomer of ALA was selected for the following reasons, 1) only the R-(+) enantiomer is endogenously synthesized and obtained through the diet, 2) the R-(+) enantiomer is more pharmacologically active and metabolically potent both in

vitro and in vivo [13-15], and 3) Na-RALA is likely to be more advantageous than other forms of ALA in terms of in vivo application due to greater water solubility and a much more favorable pharmacokinetic profile [11]. In this study, the effect of Na-RALA on CPT and paclitaxel-induced cytotoxicity was evaluated in A549 human NSCLC cells. Dose-response curves after treatment with the individual compounds for 2, 4, and 6 days revealed that, as hypothesized, Na-RALA (Figure 4) is more potent than S-lipoic acid (Figure 4). The superiority of Na-RALA cytotoxicity toward A549 NSCLC cells lends further credence to a metabolic cytotoxic mechanism of alpha lipoic acid as suggested by Wenzel et al. [9]. In other words, the higher potency of Na-RALA in increasing mitochondrial respiration (and increasing superoxide production) resulted in higher levels of cell death. It was also found that paclitaxel was the most cytotoxic compound (Figure 4). CompuSyn®3.01 analysis of the CPT/Na-RALA and paclitaxel/Na-RALA combinations revealed that interactive effects vary and depend on both the doses of the compounds and the treatment times. Comparison of the CIs at the various effect levels showed that CPT/Na-RALA combination is more favorable due to markedly lower CIs and a greater number of CIs indicative of additivity and/or synergy ($CI \leq 1$), especially after 2 and 4 days of treatment. All CIs for the paclitaxel/Na-RALA combination were indicative of antagonistic effects ($CI > 1$). DRIs for the CPT/Na-RALA combination (~0–25) were much greater than those for the paclitaxel/Na-RALA combination (~0–6). Because the DRI is a parameter that indicates the degree to which a drug dose can be reduced when used in combination with another drug and maintain an equivalent effect level, these results show that the dose of CPT can be reduced up to 22-fold when used in combination with Na-RALA. This favorable data for the CPT/Na-RALA combination

suggests that the combination deserves further evaluation. More specifically, because the lowest CIs and the highest DRIs for the CPT/Na-RALA combination occurred at 2 and 4 days and at higher effect levels (i.e., higher cytotoxicity), it will be interesting to investigate whether there exists a schedule-dependency (simultaneous treatment vs. pre- or post-treatment) for this combination and/or whether the most favorable combinatorial effects occur when the maximum level of cytotoxic induction is attempted. It should also be noted that, according to Chou, synergy at higher effect levels, as in the case of the CPT/Na-RALA combination, is more relevant to anticancer therapy [74]. This adds even further significance to the current results. An important finding in this study was that Na-RALA showed a selective cytotoxic effect for A549 NSCLC adenocarcinoma cells. "Normal" BEAS-2B lung epithelial cells were essentially unaffected after treatment with Na-RALA (Figure 7). However, longer treatment of BEAS-2B lung 430 epithelial cells with Na-RALA induced an anti-proliferative effect, although examination of cell morphology indicated a lack of cytotoxicity. Also, replacement of Na-RALA treatment medium with control DMEM medium resulted in restoration of normal rates of BEAS-2B cell proliferation (data not shown). Thus, the selective nature of Na-RALA for A549 NSCLC adenocarcinoma cells vs. "normal" BEAS-2B lung epithelial cells was twice confirmed.

Compounds displaying antioxidant and/or anti-inflammatory activities may exert a chemoprotective effect on normal cells against the toxicity of chemotherapeutic regimens [12]. To gain some insight into a potential chemoprotective effect of Na-RALA, BEAS-2B cells were also treated with CPT/Na-RALA and paclitaxel/Na-RALA combinations. It was found that Na-RALA exerted a significant chemoprotective effect

against the cytotoxicity of CPT towards BEAS-2B cells (Figure 8). On the other hand, Na-RALA failed to protect against paclitaxel-induced cytotoxicity (Figure 8). The reasons for the difference in interaction between Na-RALA and CPT or paclitaxel are beyond the scope of this manuscript. The implications of this finding are that not only can the dose of CPT be reduced up to 22-fold (corresponding to the highest DRI) and maintain an equivalent cytotoxic effect level, but that this dose reduction is accomplished with a selective agent that is benign to normal tissues and that may exert a chemoprotective effect on normal tissues exposed to the already reduced chemotherapy doses. To our knowledge, there are very few agents with this capability. Although natural compounds such as curcumin [75] from turmeric and EGCG [76] from green tea have been shown to induce a selective cytotoxic effect on cancer versus normal cells, it is well known that these compounds have critical disadvantages in terms of in vivo application, including extremely poor bioavailability, high rate of metabolism, inactive metabolic products, and rapid elimination and clearance from the body [77]. Na-RALA, on the other hand, has high bioavailability (even after oral administration), favorable pharmacokinetic parameters [11], and has active intracellular metabolic products (dihydrolipoate) that may also possess anticancer activity [78]. In addition, as mentioned previously, our lab has several successful strategies for improving the delivery and/or reducing the toxicity of CPT, including tumor-targeted bioconjugatebased and poly (ethylene glycol)-based delivery, membrane transport facilitation, and pro-drug approaches[69-73, 79, 80].

It is likely, and future studies would confirm, that simultaneous use of Na-RALA with other pharmacological or drug-delivery approaches such as ours may result in even more efficient and less toxic therapeutic strategies.

In conclusion, in the current studies, it was shown that CPT/Na-RALA is a more favorable combination than paclitaxel/Na-RALA in terms of in vitro cytotoxic effects toward A549 human NSCLC adenocarcinoma cells due to a higher likelihood of synergy/additivity and a higher potential for chemotherapy dose reduction. Minimally toxic combination therapy with CPT/Na-RALA deserves further evaluation as a chemotherapeutic strategy against NSCLC.

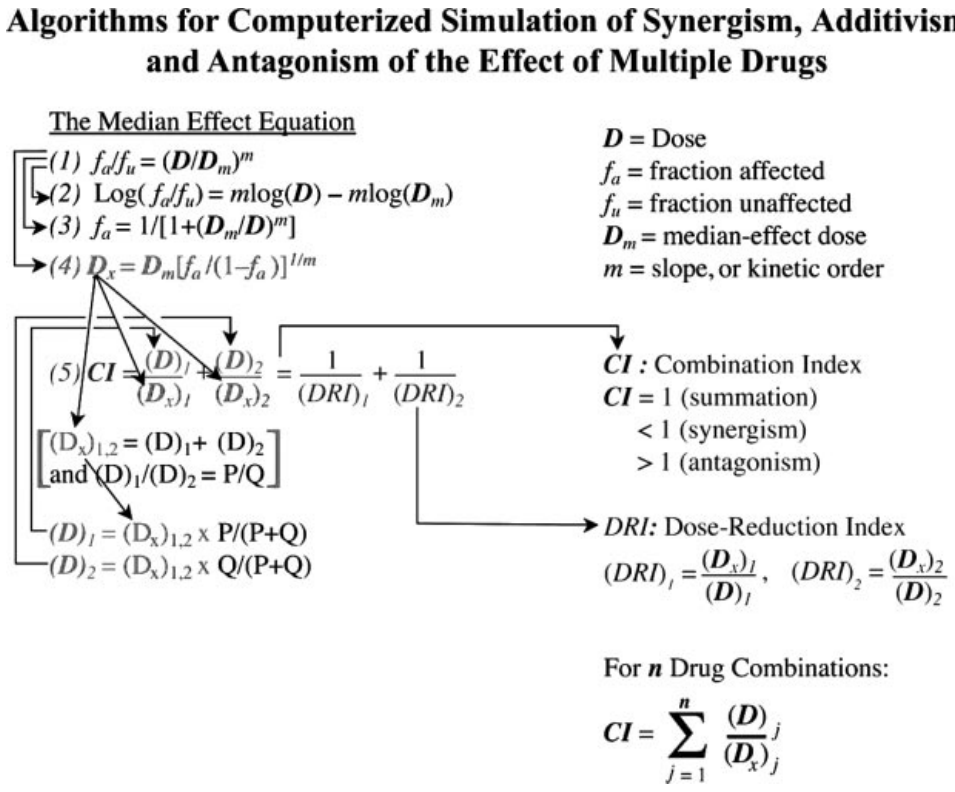

FIGURE 3 Algorithms for Simulation of Synergism, Additivism, and Antagonism of the Effect of Multiple Drugs

EC50s camptothecin, paclitaxel, sodium-R-alpha lipoate, S-lipoic acid, camptothecin/sodium-R-alpha lipoate, and paclitaxel/sodium-R-alpha lipoate after treatment of A549 NSCLC cells for 2, 4, and 6 days of treatment

	2 days	4 days	6 days
Camptothecin (nM)	23.68	14.76	7.69
Sodium-R-alpha lipoate (1) (mM)	3.12	2.21	0.40
Paclitaxel (nM)	0.0031	0.0034	0.0024
Sodium-R-alpha lipoate (2) (mM)	1.77	0.70	0.52
S-lipoic acid	—	3.56	1.54

TABLE 4 EC50s of CPT, Na-RALA, S-ALA, CPT/Na-RALA, and PXL/Na-RALA after treatment of A549 NSCLC cells for 2, 4, and 6 days of treatment.

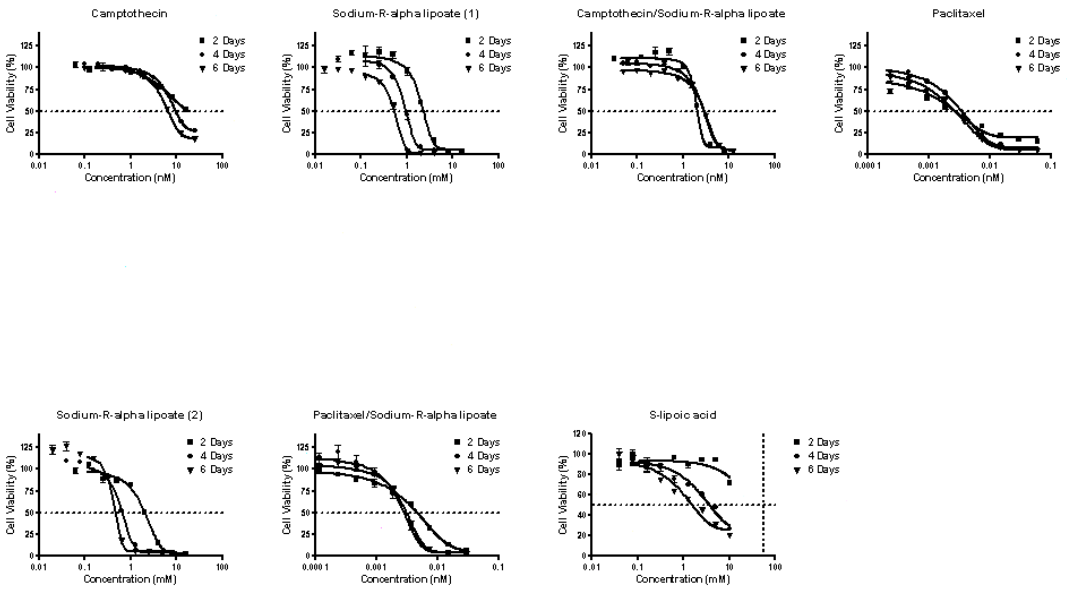

FIGURE 4 Dose-response curves of the treatments. Effect of CPT, paclitaxel, Na-RALA, S-lipoic acid, CPT/Na-RALA, and paclitaxel/Na-RALA on A549 cell viability after 2, 4, and 6 days of treatment. Cell viability was assessed using the MTT assay. Individual points within dose-response curves were expressed as mean ± standard error of mean. Differences between dose-response curves within each plot were found to be statistically significant ($P<0.05$).

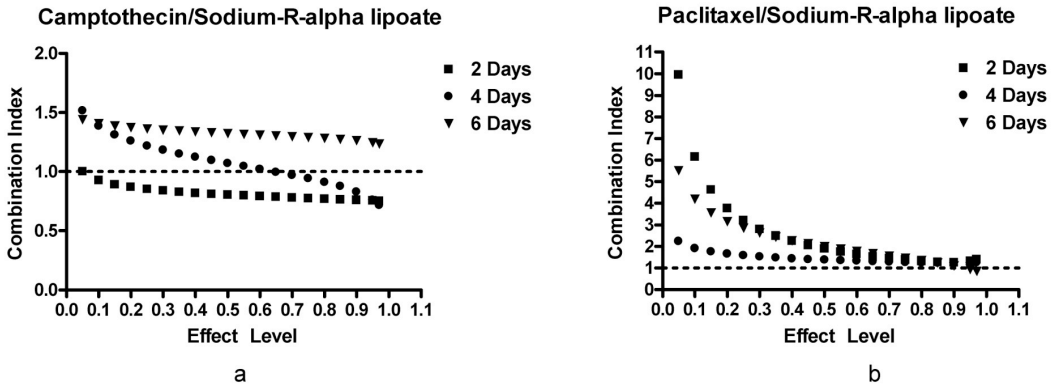

FIGURE 5 CIs of combination treatments. CIs as a function of effect level of the campothecin/sodium- R-alpha lipoate and paclitaxel/sodium-R-alpha lipoate combinations after treatment of A549 cells for 2, 4, and 6 days. CIs determine the type of interaction. Additive (CI=1); Synergistic (CI<1); Antagonistic (CI>1).

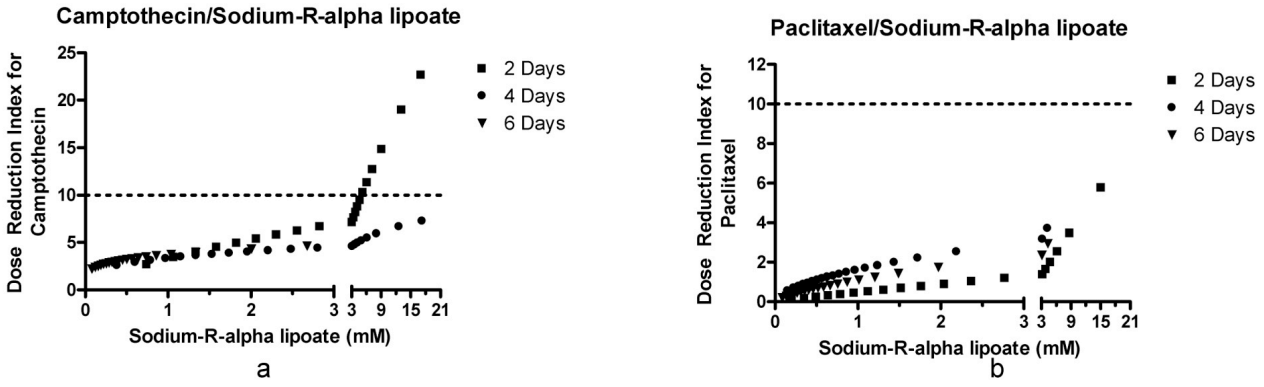

FIGURE 6 DRIs of the combination treatments. DRIs for camptothecin and paclitaxel when combined with sodium-R-alpha lipoate. The DRI is a parameter that indicates the degree to which a drug dose can be reduced when used in combination with another drug and maintain an equivalent effect level.

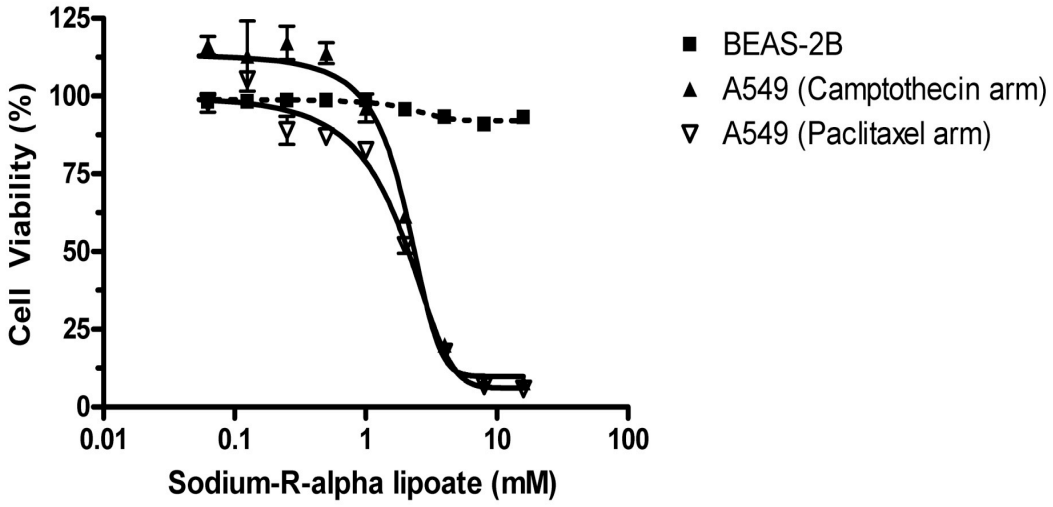

FIGURE 7 Effect of sodium-R-alpha lipoate on BEAS-2B cells. Representative data of the effect of sodium-R-alpha lipoate on A549 NSCLC and BEAS-2B 'normal' lung epithelium cell viability after treatment for 2 days.

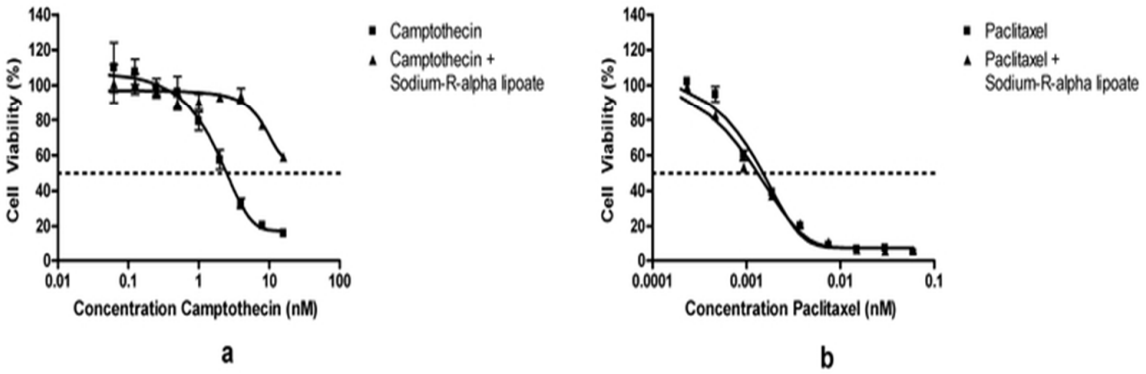

FIGURE 8 Effect of camptothecin/sodium-R-alpha lipoate and paclitaxel/sodium-R-alpha lipoate on BEAS-2B cells. Cell viability of BEAS-2B 'normal' lung epithelial cells after treatment with CPT/Na-RALA or paclitaxel/Na-RALA for 2 days.

5. SPECIFIC AIM 2

Specific Aim 2: Evaluate the effects of CPT, Na-RALA, and combinations thereof on in vitro hallmarks of cancer, namely migration, invasion, senescence, and angiogenesis.

Hypothesis: A combination of CPT and Na-RALA will have potent effects on the in vitro hallmarks of cancer, and the combination will be more efficacious than CPT alone

5.1 INTRODUCTION

Lung cancer is the most common cause of cancer-related mortality among both men and women in the United States and worldwide [1, 26, 53]. It is also one of the most common cancers in both men and women in the United States. NSCLC is by far the most prevalent type of lung cancer, accounting for nearly 85% of all lung cancer cases. With a 5-year survival rate of ~15% in the United States and ~8% in Europe and the developing world, NSCLC remains among the deadliest cancers despite current therapeutic options [1, 2, 26, 53]. Thus, more effective therapeutic strategies are urgently needed. Early-stage NSCLC presents with vague and variable symptoms [19], causing most diagnoses to occur at advanced stages of the disease. At this point, surgical options no longer offer effective outcomes and chemotherapy becomes first-line therapy [20]. Thus, improvement of current chemotherapeutic regimens is highly sought after.

"The Hallmarks of Cancer", the seminal article published by Douglas Hanahan and Robert Weinberg in 2000 [81], aimed to define cancer by reviewing the various

hallmarks that characterize the disease. Those hallmarks are: (1) cancer cells stimulate their own growth; (2) they resist inhibitory signals that might otherwise stop their growth; (3) they resist their own programmed cell death (apoptosis); (4) they stimulate the growth of blood vessels to supply nutrients to tumors (angiogenesis); (5) they can multiply forever; and (6) they invade local tissue and spread to distant sites (metastasis). In 2010 [82], the authors published an updated version of the article that added two new hallmarks: (7) abnormal metabolic pathways and (8) evading the immune system. From a therapist's perspective, "The Hallmarks of Cancer" emphasizes the need for prospective anti-cancer strategies to simultaneously target multiple hallmarks of cancer to be most successful. Combination strategies, i.e. the use multiple compounds for cancer therapy, may offer an effective solution. In essence, combination strategies, due to the inclusion of compounds with possibly divergent mechanisms, aim to produce an additive or synergistic therapeutic response through an enhanced cytotoxic effect and to simultaneously target multiple hallmarks of cancer.

We have previously hypothesized that a combination of CPT (CPT) and Na-RALA (Na-RALA) would be an effective combination for the treatment of NSCLC. CPT is on the list of NCI drugs that has previously failed due to toxicity and formulation issues despite remarkable therapeutic potential. To resolve this issue and exploit the potential of CPT, we are currently developing composite gel microparticles (CGMPs) comprising nanoparticles (NPs) for selective delivery of CPT to the lung [83]. In addition, our laboratory has extensive experience with the drug and it's pro-drugs [69, 72, 73, 79]. In particular, our laboratory has previously shown that lung targeting of a CPT pro-drug (CPT-norvaline), via passive entrapment of rigid microparticles can reduce

therapeutic doses of CPT 10-fold in a rat orthotopic lung cancer model. Na-RALA, the sodium salt of the endogenously-synthesized and diet-obtained R-enantiomer of the essential metabolic cofactor alpha lipoic acid, was deemed a possibly effective compound for a combination strategy with CPT due to the following reasons: 1) it targets the metabolic abnormality of cancer [9, 63, 66], i.e. Warburg Effect- the preferential use of aerobic glycolysis in lieu of oxidative phosphorylation (one of the hallmarks); 2) it has shown anti-cancer effects in vitro and in vivo [6-9]; 3) due to it's metabolic-targeting effect, it has shown evidence for cytotoxic selectivity towards cancer cells (i.e. benign toward normal cells) [9]; 4) it has shown matrix metalloproteinase (MMP)-inhibitory activity that may hinder metastasis[84]; and 5) it is highly water soluble, bioavailable, and can reach high, therapeutic plasma concentrations even via oral administration [11].

In a previous study, we examined the effects of CPT, Na-RALA, and their combination at various time points and concentrations on A549 human lung cancer cells and "normal" BEAS-2B lung epithelial cells. We concluded that some beneficial aspects of this combination are: 1) it produces concentration-dependent, synergistic cytototoxic effects on A549 human NSCLC cells, allowing a dose reduction of CPT and/or it's delivery system and thus lowered toxicity; 2) Na-RALA was selective for A549 lung cancer cells since the compound was non-toxic towards "normal" BEAS-2B lung epithelial cells; (3) Na-RALA imparted a chemoprotective effect on "normal" BEAS-2B lung epithelial cells against the toxic effects of CPT.

As mentioned previously, the cytotoxic synergy shown by CPT/Na-RALA is promising. However, it is now well known that cytotoxic chemotherapy that relies exclusively on the reduction of cancer cell numbers is inefficacious. Metastasis, for

example, is the ultimate cause of death in up to 90% of patients [85], and the induction of senescence to induce cytostasis maybe an excellent adjunctive to cytotoxic strategies. Also, anti-angiogenic therapies across a wide variety of cancers, including NSCLC, have highlighted the role of this process in disease progression. For this reason, herein we continue our investigation of this combination strategy in the framework of the hallmarks of cancer, namely, migration, invasion, senescence, and angiogenesis.

5.2 MATERIALS AND METHODS

Cell Culture

A549 human NSCLC adenocarcinoma cells (American Type Culture Collection, Rockville, MD) were cultured and passaged in Dulbecco's modified eagle medium (DMEM) supplemented with 10% fetal bovine serum (FBS) and 100 U/ml penicillin- 100 µg/ml streptomycin. Human umbilical vein endothelial cells (HUVEC's), a human umbilical endothelial cell line, were purchased from ATCC. The cells were maintained in DMEM/F-12 medium supplemented with 2.438 g/l sodium bicarbonate (Invitrogen), 10% FBS (Biowest), 0.1 mg/ml heparin (Sigma), 0.03 mg/ml ECGF (Sigma), and 100 U/ml penicillin- 100 µg/ml streptomycin. Cell lines were maintained in incubator at 37°C and 5 % CO2.

Cell Migration Assay

A549 cells were grown to confluence in 100 mm cell culture dishes. Confluence was confirmed with microscopy and the confluent cell sheets were then scratched with a 100 µl pipette tip to create a "wound" that extends the diameter of the cell culture dish.

Wound sizes were measured to ensure equivalence of the pre-migration conditions for all treatment groups. Dishes of A549 cells were treated with DMEM/solvent controls, CPT (10 nM), Na-RALA (500 μM), and CPT (10 nM)+Na-RALA (500 μM). The "healing" of the wound, i.e. the migration of the cells back into the wound, was monitored for 1, 2, 3, and 4 days with phase contrast microscopy. Images were taken at 0, 1, 2, 3, and 4 days and edited for clarity.

Cell Invasion Assay

Cell invasion was evaluated using a fluorometric, 24-well, 2-chamber assay from EMD Millipore (Billerica, MA). The assay was conducted according to manufacturer's instructions. Briefly, A549 cells were starved in T75 cell culture plates for 24 hours prior to plating in the inserts of the 24-well invasion chamber. A549 cells were treated with DMEM/solvent controls, CPT (10 nM), Na-RALA (500 μM), and CPT (10 nM)+Na-RALA (500 μM). DMEM with 10% FBS (the chemoattractant) was placed in the bottom wells of the invasion chamber. Invading cells degrade the basement membrane (ECMatrix™), migrate through 8 μm pores, and attach to the bottom of the membrane. Non-invading cells will not be able to degrade the basement membrane and remain above. Invading cells are detached from the bottom of the membrane into the bottom wells of the invasion chamber. A visual determination of the invading cells was performed with phase contrast microscopy. Following cell lysis, a quantitative determination was also performed with CyQuant GR fluorescent dye at 480/520 with a fluorescence plate reader.

MMP Inhibition Assay

A generic MMP assay was used to evaluate the effects of treatment on MMP-2 and MMP-9 activity according to the manufacturer's instruction (Anaspec, Fremont, CA). Briefly, cells were treated in triplicate groups (24-well plates) with solvent control, MMP inhibitor (GM6001, 20 μM), CPT (10 nM), Na-RALA (500 μM), and CPT (10 nM)+Na-RALA (500 μM) for 24 hours. Cells were lysed on ice for 10 min using 1.0 mL lysis buffer per well (0.5% (v/v) Triton X-100 in 0.1 mol/L Tris-HCl (pH 8.1)) and removed with a sterile plastic cell scrapper. Cell lysates were spun at 10,000 rpm using an Allegra 2502 bench-top centrifuge (Beckman Coulter). Supernatants were incubated with trypsin (10 ug/mL, for MMP-9) or AMPA (1 mM, for MMP-2), to activate pro-MMPs immediately before MMP substrate addition. MMP substrate was added for 1 hour (MMP-2) or 2 hours (MMP-9) at 37°C. 50 μL samples were added to 96-well plates and absorbance was measured at in a Tecan plate reader.

Senescence Assay

Senescence was detected using a β-galactosidase senescence kit according to manufacturer's instructions (Biovision, Milpitas, CA). Briefly, A549 cells were plated in 12-well plates and underwent treatment with CPT (10 nM), Na-RALA (500 μM), and CPT (10 nM)+Na-RALA (500 μM) for 24 hours. Cells were fixed and then stained overnight. Senescent cells were identified by the development of a dark blue color using phase contrast microscopy.

Angiogenesis Assay

Matrigel® (0.03 ml) was added to a pre-chilled 96-well plate and left in the incubator for 30 minutes. Thereafter, various loads of HUVECs were transferred in 0.1 ml culture medium to the pre-coated wells. After 24 hours, the cells were photographed with phase contrast microscopy. Tube formation was then analyzed with Angiogenesis Analyzer for ImageJ (version 1.49h). The optimal cell density for tube formation was determined to be 1.5×10^4 cells/well. MTT assay was used to determine maximum non-toxic concentrations (data not shown) to be used for angiogenesis inhibition. Non-toxic concentrations of CPT, Na-RALA, and combinations thereof were then explored to determine effects on tube formation as quantified by total master segment length.

Statistical Analysis

GraphPad Prism® (La Jolla, CA) was used to conduct statistical analyses for all assays. Briefly, for the migration assay, two-way ANOVA in conjunction with Bonferroni multiple comparisons test, was used to determine statistical differences within each treatment group across time points and between all groups for each time point. For the angiogenesis assay, one-way ANOVA in conjunction with Dunnett's multiple comparisons test was used to determine statistical differences between any two groups. For all other assays, one-way ANOVA, in conjunction with Tukey's multiple comparisons test, was used to determine statistical difference between any two groups. Bar graphs are expressed as mean ± standard error of mean. The limit for statistical significance was set at $P<0.05$.

5.3 RESULTS

Effects of Treatment on A549 Cell Migration

It is well known that A549 cells are capable of migrating under basal conditions. Therefore, we investigated cell migration using the wound healing assay under control and treatment conditions. We found that untreated A549 cells rapidly migrated, nearly filled the gap by Day 2 (~10% of original size), and completely filled the gap by Day 3. CPT (10 nM) treatment slightly slowed cell migration compared to control, maintaining the gap at 23% and 14% of its original size at 2 and 3 days, respectively. On the other hand, Na-RALA (500 μM), both alone and in combination with CPT (10 nM) markedly inhibited cell migration. Combo treatment had a slightly more potent anti-migratory effect than Na-RALA that was apparent at 2 days (~65% vs. 57% of original wound size) and maintained through day 3, although without a statistical difference (Figure 9).

Effects of Treatment on A549 Cell Invasion

With 10% FBS-supplemented DMEM acting as the chemoattractant in the dual chamber invasion assay, we found that untreated A549 cells were very capable of invading through the basement membrane and migrating to the bottom wells, as shown by both phase contrast microscopy (Figure 10) and the high level of fluorescence (Figure 11). CPT (10 nM)-treated cells showed no statistically significant effect on cell invasion compared to control cells as determined by quantitative fluorescence testing, although a slight inhibitory trend is apparent from representative phase contrast images (Figure 10). Na-RALA (500 μM) showed a ~63% inhibition of invasion compared to solvent control

cells, and this effect was statistically different from all other groups. Combo treatment showed a ~80% inhibition of invasion compared to control cells, and this effect was statistically different from all other groups.

Effects of Treatment on MMP-2 and MMP-9 activity in A549 Cells

MMP-2 and MMP-9 activities for all treatment groups were normalized to non-treated control levels. MMP-2 and MMP-9 activities in positive control-treated (MMP inhibitor GM6001, 20 μM) A549 cells were potently inhibited (~7% and 9% of control values, respectively) showing statistical significance compared to control, CPT, Na-RALA, and combo groups. Treatment with CPT (10 nM) alone was inefficacious in inhibiting MMP-2 or MMP-9 activity in A549 cells, with no statistical difference compared to the control group. On the other hand, treatment with Na-RALA, alone and in combination with CPT inhibited MMP-2 and MMP-activity. Sole treatment with Na-RALA inhibited MMP-2 activity by ~8% and MMP-9 activity by ~42%. Combination treatment with CPT and Na-RALA inhibited MMP-2 activity by 24% and MMP-9 activity by 59% (Figure 12).

Effects of Treatment on Senescence

Control, CPT (10 nM), and Na-RALA (500 μM) treated A549 cells showed almost no senescence induction at 24 hours. Interestingly, combo treatment with CPT and Na-RALA showed a marked synergistic effect in senescence induction (up to 7-fold) that

was readily apparent from phase contrast images (Figure 13), and cell count (Figure 14) was statistically different from all other treatment groups.

Effect of Treatment on Angiogenesis

Total master segment length of tubes formed by HUVECs was used as a parameter for angiogenesis. Treatment with CPT (0-0.5 μM) alone showed no inhibition of angiogenesis at any concentration. Treatment with Na-RALA alone (0-0.6 mM) significantly inhibited angiogenesis at 0.6 mM (~90% inhibition), but showed no effects at lower concentrations. Treatment with CPT/Na-RALA inhibited angiongesis at two combinations: CPT 0.25 μM/Na-RALA 0.3 mM, ~40% inhibition; CPT 0.5 μM/Na-RALA 0.6 mM, 90% inhibition (Figure 15).

5.4 DISCUSSION

Lung cancer is among the most common and deadly cancers in the world, killing more people than breast, prostate, and colorectal cancers combined [1, 26, 53]. It is estimated that 1.37 million people worldwide die of the disease annually. NSCLC accounts for the majority of lung cancer cases and thus a remains a focus in the search for more effective treatments. Approximately 40% of patients diagnosed with NSCLC have unresectable stage III disease or medically inoperable disease, implicating the importance of non-surgical treatment options and better diagnostic procedures. Cytotoxic chemotherapy and radiation remain the first-line, non-surgical treatments for NSCLC, yet

the still-high levels of mortality and morbidity of the disease point to the shortcomings of these approaches. Perhaps the reason is that the traditional reliance on cytotoxic treatment strategies assumes that complete cellular destruction of tumors optimizes the potential for patient survival. However, these approaches not only fail to produce complete cell death within a solid tumor and can cause severe side effects in patients, but also overlook the complexity and diversity of cellular mechanisms occurring in cancer as highlighted in the groundbreaking article "The Hallmarks of Cancer". Briefly, those hallmarks are: (1) cancer cells stimulate their own growth; (2) they resist inhibitory signals that might otherwise stop their growth; (3) they resist their own programmed cell death (apoptosis); (4) they stimulate the growth of blood vessels to supply nutrients to tumors (angiogenesis); (5) they can multiply forever; (6) they invade local tissue and spread to distant sites (metastasis); (7) abnormal metabolic pathways; and (8) evading the immune system.

An alternative strategy is the use of combinations that not only display synergy or additivity in cell killing for primary tumor eradication, but also effect multiple hallmarks of cancer in order to prevent progression and eventual mortality of disease. For example, pro-senescence [86, 87], anti-metastatic [88, 89], and anti-angiogenic [90, 91] approaches are gaining considerable attention in cancer chemotherapy due to the critical roles of these processes in cancer progression and mortality. Within this framework, we have previously hypothesized that a combination of CPT and Na-RALA would be a novel therapeutic strategy for the treatment of NSCLC. CPT is a cytotoxic quinolone alkaloid isolated from the bark and stem of *Camptotheca Acuminata[4]*. The drug's primary mechanism of action is inhibition of topoisomerase I, which prevents DNA unwinding

and leads to cell death. As mentioned previously, despite CPT's remarkable therapeutic potential, the drug has failed due to formulation and toxicity issues. However, we are also developing a CGMP-NP delivery system that selectively targets the lungs and avoids off-target exposure [83], Na-RALA is the sodium salt of the active R-enantiomer of alpha lipoic acid, which has shown promising anti-cancer, antioxidant, anti-inflammatory, and MMP-inhibitory activities. In addition, due to it's metabolic-targeting effect [9], it exploits metabolic abnormalities in cancer (i.e. Warburg Effect) [64, 65] and has shown evidence for cytotoxic selectivity towards cancer cells [9, 92]. Additionally, the Na-RALA form is ideal due to greater metabolic potency of the R- vs. S-enantiomer, greater water solubility, and a much more favorable pharmacokinetic profile. In a previous study, we showed additive or synergistic cytotoxic effects of a combination of CPT and Na-RALA towards A549 human NSCLC adenocarcinoma cells [92]. In addition, it was shown that Na-RALA is selective towards A549 cells vs. normal BEAS-2B lung epithelial cells and that Na-RALA protects normal lung epithelial cells against exposure to CPT [92]. In this study, we continued our evaluation of this combination and examined its effects on certain hallmarks of cancer, namely migration, invasion, senescence, and angiogenesis.

Metastasis is the spread of cancer cells from a primary tumor to different organs. It is estimated that 50 percent of NSCLC deaths today are due to metastatic disease (to the bone, brain, and liver) and/or its complications. Tumor cell migration and invasion are essential prerequisites for metastasis formation. In this study, the effect of Na-RALA, CPT, and their combination on A549 migration and invasion were evaluated. A549 cells rapidly migrated as expected and healed the "wound" by day 3. Although CPT only

slightly inhibited A549 cell migration, Na-RALA and combo treatment markedly attenuated A549 cell migration as shown by relatively large "wound" sizes at days 2 and 3, with no statistical difference between the two treatments (Figure 9). Similarly, CPT-treated cells showed no effect on cell invasion compared to control cells, whereas Na-RALA and combo treatment showed a ~63% and ~80% inhibition of invasion, respectively, compared to controls (Figures 10 and 11). Interestingly, the inhibitory effects of combo treatment were statistically greater than Na-RALA treatment alone, suggesting additivity or synergy in the anti-invasion effect since treatment with CPT alone showed no statistically significant effect.

The inhibitory effects of the treatment on cell invasion, particularly of Na-RALA, prompted us to investigate the mechanism responsible. Matrix metalloproteinases (MMPs) belong to a family of secreted or membrane-associated zinc endopeptidases capable of digesting extracellular matrix components and processing certain bioactive mediators. To date, 24 MMP genes have been identified in humans [93, 94]. MMPs play a central role in metastatsis, invasion, and angiogenesis, and inhibitors thereof are currently undergoing clinical trials for cancer therapy [94]. In particular, MMP-2 and MMP-9 are the most frequently implicated in metastatic disease and have been detected in human NSCLC samples [95]. To gain insight into the mechanisms responsible for the anti-invasion effect of the treatment, we measured the activities of the MMP-2 and MMP-9 in A549 cells in response to treatment. It was shown that CPT alone was inefficacious in inhibiting MMP-2 or MMP-9. On the other hand, treatment with Na-RALA, both alone and in combination with CPT, inhibited MMP-2 and MMP-activity. Na-RALA inhibited MMP-2 activity by ~8% and MMP-9 activity by ~42%. Combination treatment

with CPT and Na-RALA inhibited MMP-2 activity by 24% and MMP-9 activity by 59% (Figure 12). Similar to the results of treatment on invasion, the greater potency of combo treatment compared to sole treatment with CPT or Na-RALA suggests the involvement of additivity or synergy. Our results suggest that MMP-2 and/or MMP-9 inhibition are at least partially responsible for the anti-invasion effect of our treatment. It should be mentioned that we are not the first to observe an MMP-inhibitory activity of ALA in cancer cells [84].

The induction of senescence, the permanent disabling of the proliferative capacity of cancer cells without inducing cell death, is a new frontier in cancer drug development. Initial studies utilizing pro-senescence treatments have yielded promising preliminary results, suggesting that these treatments may be as effective as cytotoxic therapies in cancer treatment and with fewer and less severe side effects. In addition, this approach to treatment may provide a more realistic goal for the chronic management of cancers [86, 87, 96]. We showed here that although treatment with CPT or Na-RALA alone showed no effect on senescence, combo treatment with both CPT and Na-RALA showed a marked effect in senescence induction (up to 7-fold). The difference in magnitude in senescence induction (from null to 7-fold) between treatment with CPT or Na-RALA alone and combo treatment suggests that the compounds interact synergistically (Figures 13 and 14).

Angiongenesis, the formation of new blood vessels, is a process that involves the migration, invasion, and growth of endothelial cells. Angiongesis plays a critical role in cancer progression as the formation of new blood vessels is necessary to promote growth of both primary tumors and metastatic lesions. Angiongenesis inhibitors, including the

VEGF antibody bevacizumab (Avastin®), are already being used in the clinic to treat cancers including NSCLC. In this investigation, it was shown that sole treatment with the chemotherapeutic agent CPT had no inhibitory effects on angiogenesis. However, a high concentration of Na-RALA (0.6 mM) or a combination of CPT/Na-RALA readily inhibited angiogenesis as shown by decreased tube segment length (Figure 15).

From both therapeutic and pharmacological perspectives, it is becoming increasingly obvious that standalone cytotoxic chemotherapy has thus far failed in the war on cancer generally and on NSCLC specifically. Said treatments not only fail to eradicate primary tumors, but also neglect the complex mechanisms responsible for disease progression and induce severe side effects in patients. Our combination strategy with CPT and Na-RALA offers a dose-reduction of cytotoxic CPT and/or its delivery system, exploits synergy for cytotoxicity and primary tumor eradication, addresses multiple hallmarks of cancer, and with lower/targeted doses of CPT, has the potential to be used in the chronic management of NSCLC.

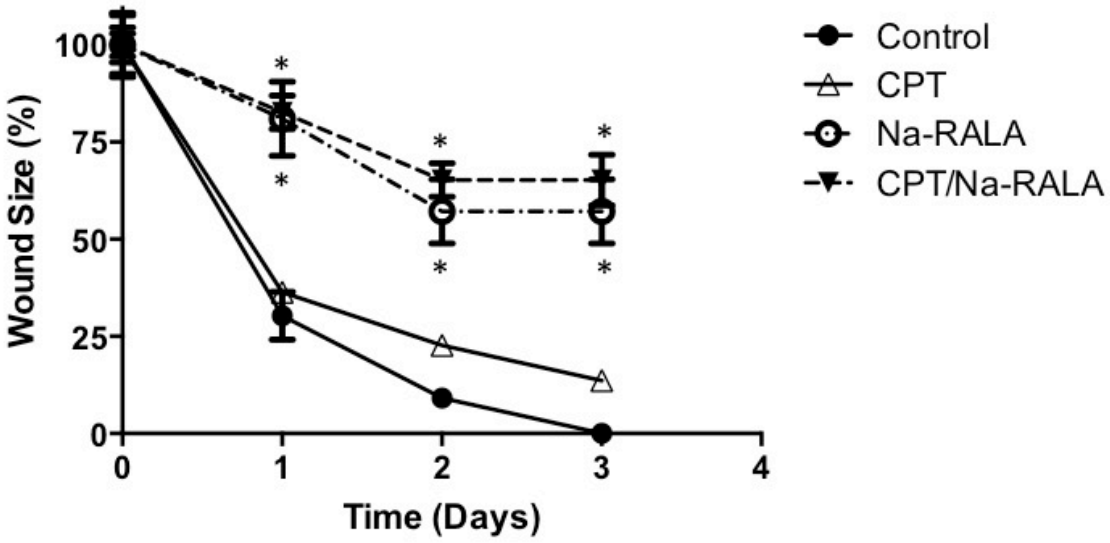

FIGURE 9 Wound Healing Assay. A549 cell migration vs. time after treatment with CPT, Na-RALA, and CPT/Na-RALA. Groups marked with * are significantly different from Control and CPT groups, $p<0.05$.

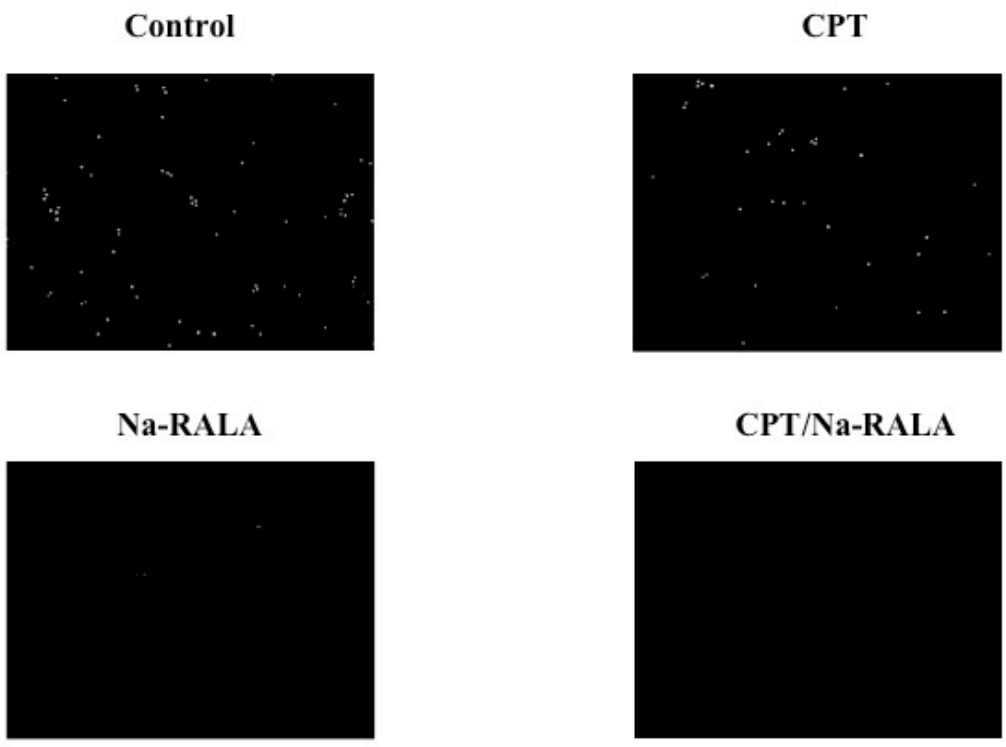

FIGURE 10 Cell Invasion Assay. Representative phase-contrast microscopy images of invading A549 cells after treatment with CPT, Na-RALA, and combo (CPT/Na-RALA) after 24 hours.

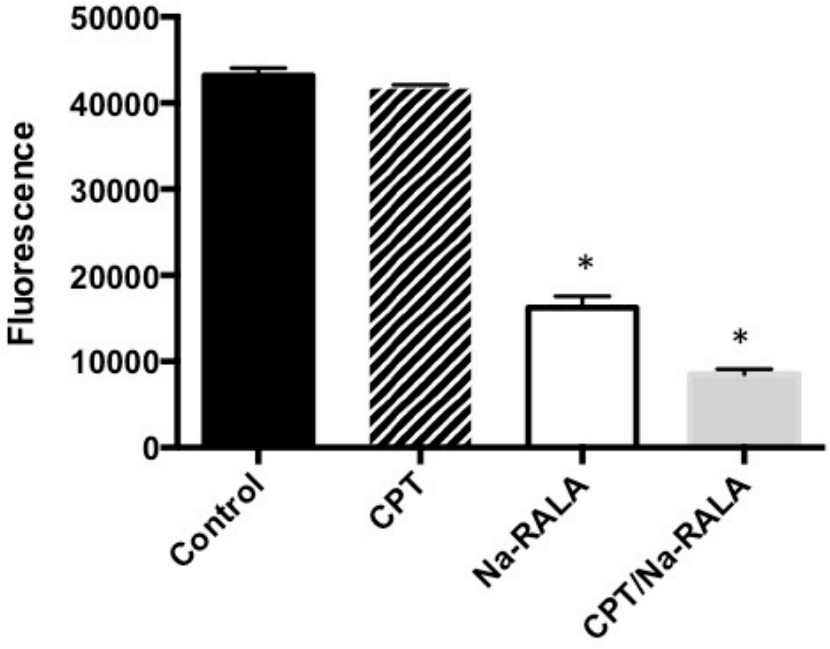

FIGURE 11 Cell Invasion Assay. Fluorescence levels as a quantitative indication of invading A549 cells after treatment with CPT, Na-RALA, and CPT/Na-RALA for 24 hours. Data are means ± SEM (n=3 for each group). Groups marked with * are significantly different from all other groups, $p<0.05$.

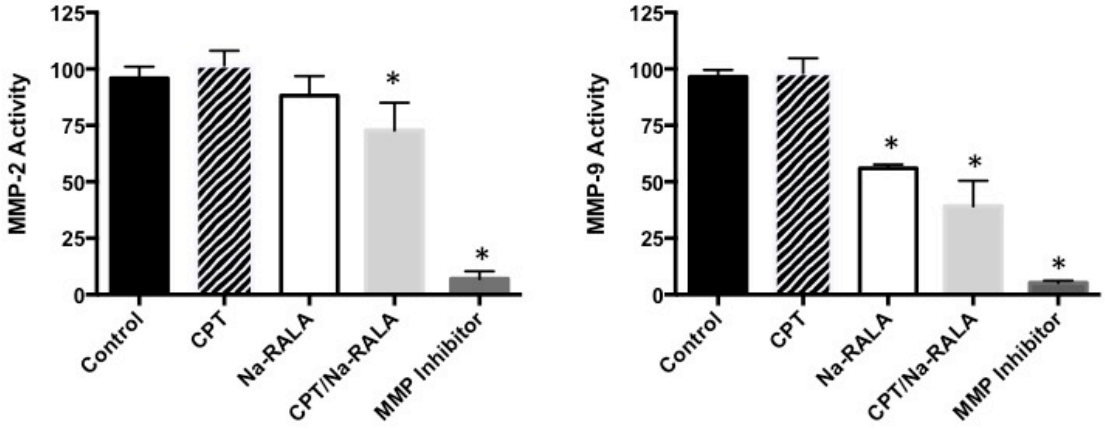

FIGURE 12 MMP-2 and MMP-9 activity of A549 cells after treatment with CPT, Na-RALA, and CPT/Na-RALA) for 24 hours. Data are means ± SEM (n=3 for each group). Groups marked with * are significantly different from all other groups, $p<0.05$.

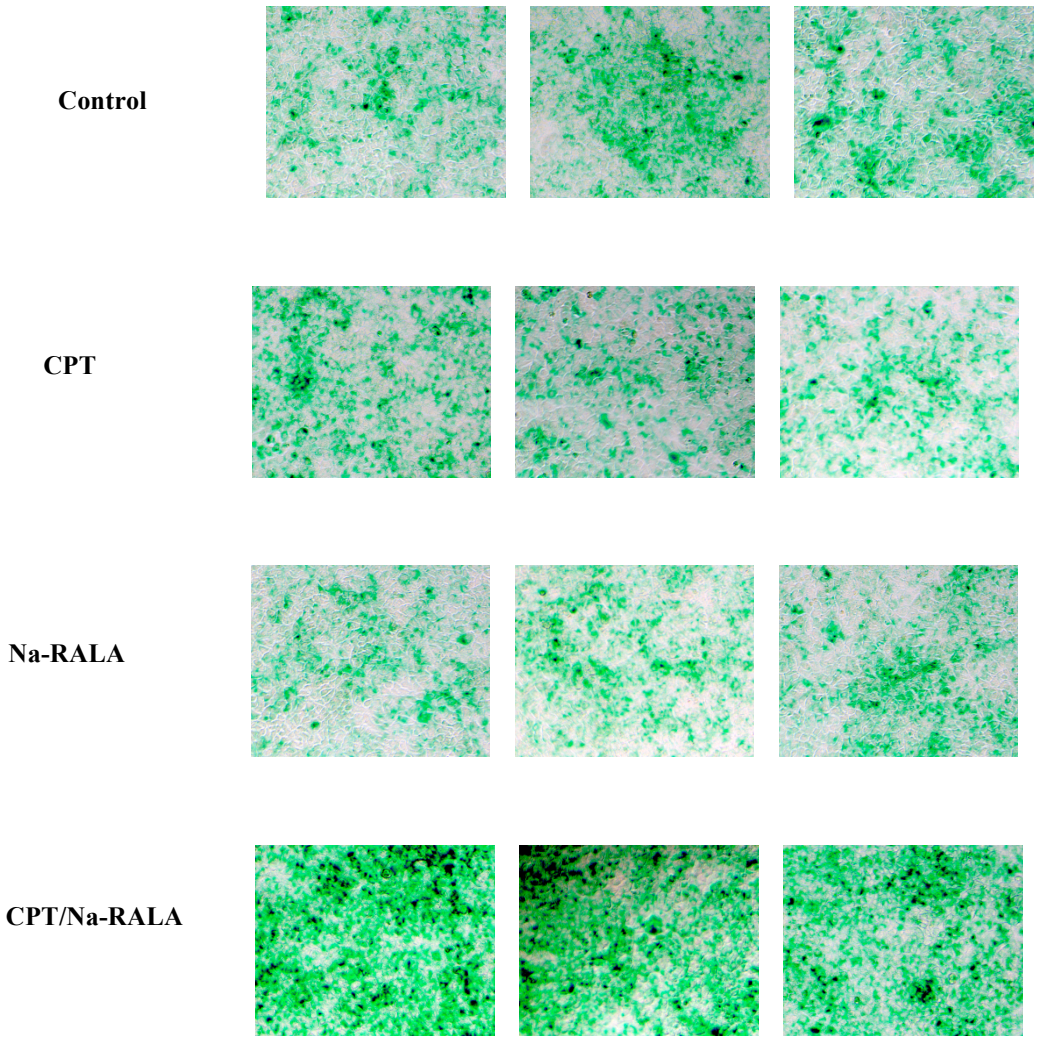

FIGURE 13 Senescence Assay. Representative phase-contrast microscopy images of senescent (dark color) A549 cells after treatment with CPT, Na-RALA, and combo (CPT/Na-RALA) for 24 hours. n=3 for all groups.

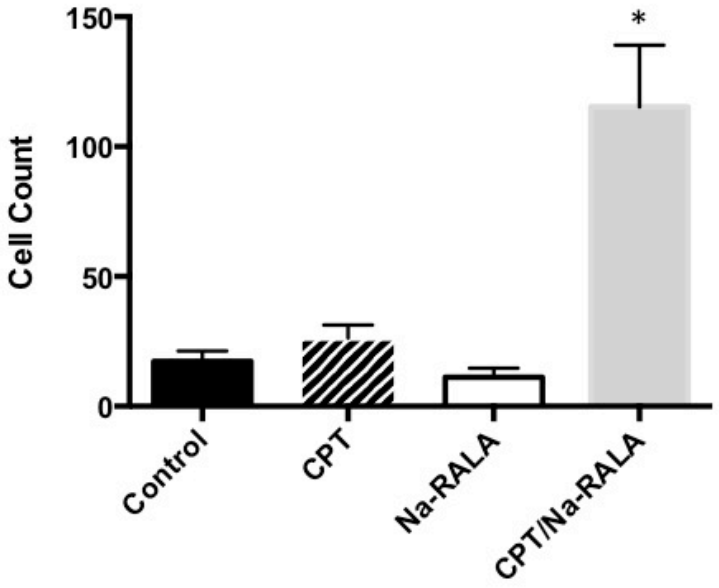

FIGURE 14 Ssenescence Assay. Cell count of senescent A549 cells in representative phase-contrast microscopy images after treatment with CPT, Na-RALA, and CPT/Na-RALA after treatment for 24 hours. Data are means ± SEM (n=3 for each group). Groups marked with * are significantly different from all other groups, $p<0.05$.

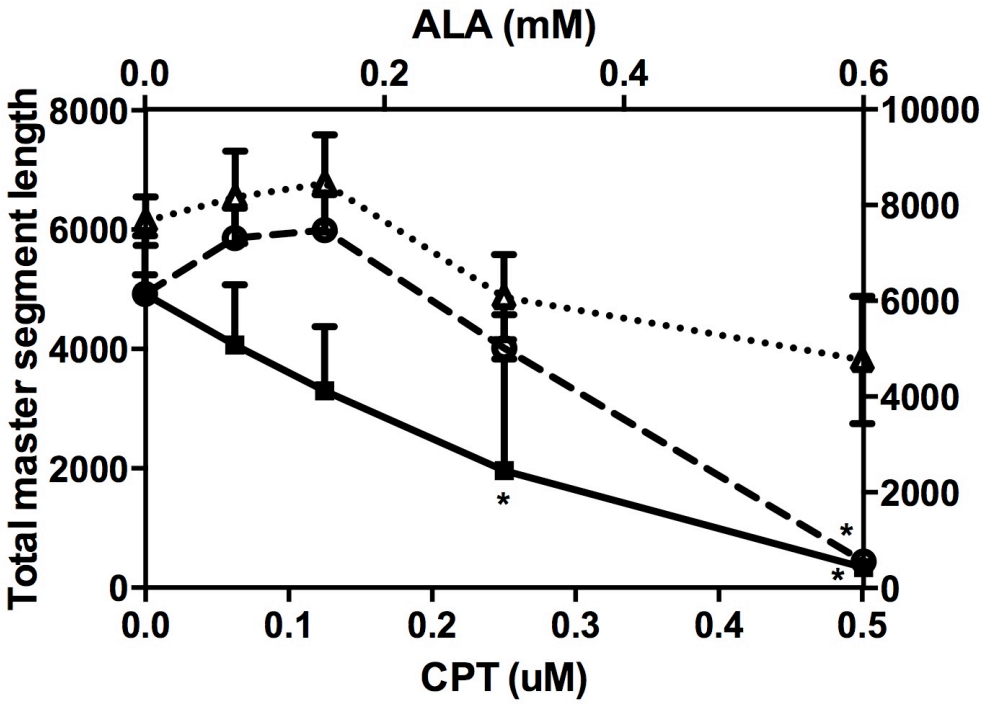

FIGURE 15 Angiogenesis Assay. Total master segment length was used as a parameter for angiogenesis. Traingle: CPT, Circle: Na-RALA, Square: CPT/Na-RALA. Groups marked with * are significantly different from all from other groups, $p<0.05$.

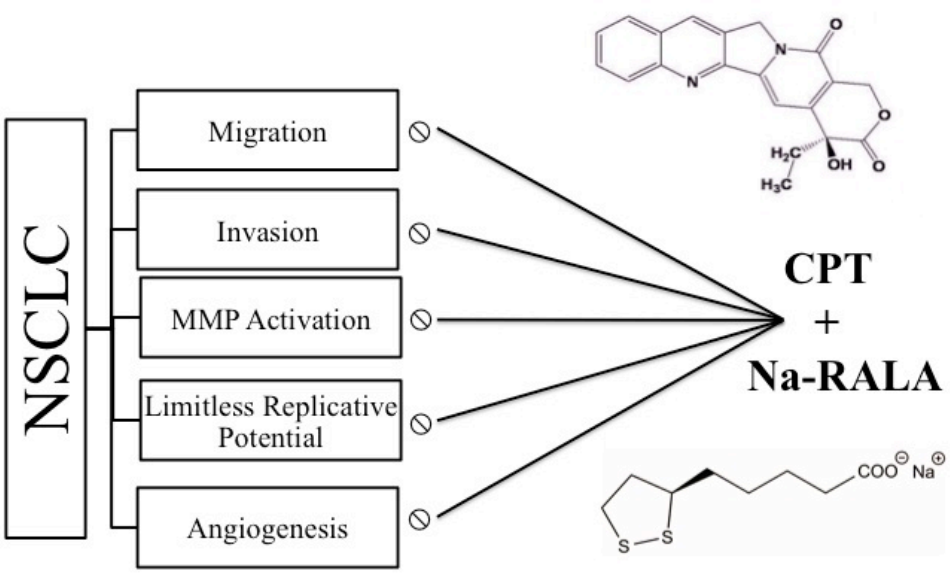

FIGURE 16 Schematic Diagram of the Effects of CPT/Na-RALA on Hallmarks of NSCLC.

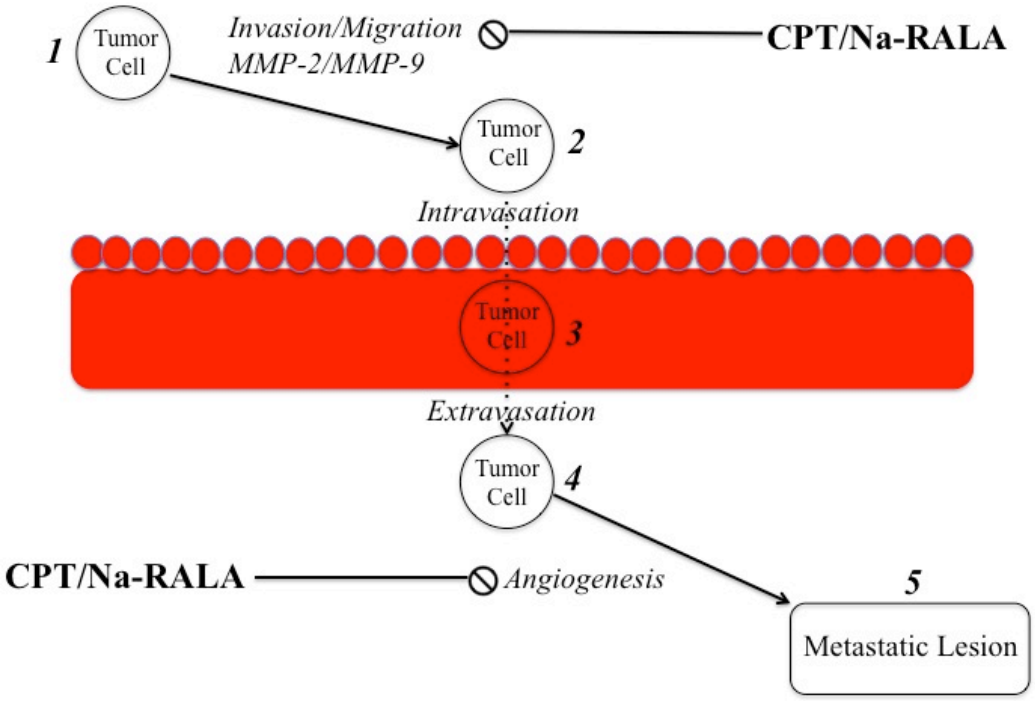

FIGURE 17 Effects of CPT/Na-RALA on the sequential steps of the metastasis cascade.

6. SPECIFIC AIM 3

Specific Aim 3: Develop a orthotopic xenograft mouse model of NSCLC for preliminary in vivo evaluation of the CPT/Na-RALA combination.

Hypothesis: The model displaying primary tumor onset and metastasis incidence in the framework of time and practicality will be used for the preliminary evaluation of the CPT/Na-RALA combination.

6.1 INTRODUCTION

Experimental model systems are critical to gain insights into lung cancer mechanisms and signaling pathways, and to evaluate the efficacy of novel treatments. A variety of animal models for lung cancer have been developed to meet the needs of research. Anatomic and physiologic similarity of the mouse to humans, excellent availability and variety in colonies, along with ease of mouse genome manipulation, make the mouse an ideal system to model human diseases including lung cancer [97, 98].

Many efforts have been made to produce transgenic mouse strains to mimic lung cancer onset caused by prominent molecular abnormalities (eg. *MYC, Ras, EGFR*, etc) in lung cancer. The transgenic models have the advantages of allowing the study of the roles of specific genes and corresponding pathways. However, such models still do not fully recapitulate the complexities of human lung cancer.

Conventional lung cancer models inoculate murine or human lung cancer cell lines into immunocompetent or immunodeficient mice. Based on the origin of the cancer cell line and the mouse recipients, the conventional models can be categorized into

allograft and xenograft models. Allograft models inoculate murine cell lines into corresponding mouse strains/stocks. A well-known example of allograft model is the injection of Lewis Lung Carcinoma cells, a murine lung cancer cell line, into C57 mouse. Xenograft models involve the injection of human cancer cells into immunodeficient animals. In these models, the location of the inoculum categorizes them into orthotopic and heterotopic lung cancer models. In orthotopic models, the cancer cell inoculum is in the natural position, whereas in hertorotopic models, it is not. The most frequently used heterotopic models involve the injection of cancer cells subcutaneously. In this model, lung cancer cells form a tumor subcutaneously at the site of injection. Another widely used heterotopic model is the intravenous model. This model injects tumor cells intravenously to mimic extensive metastasis. To achieve higher incidence of bone metastasis, tumor cells can be injected into the left cardiac ventricle to bypass the lung filtration. Direct injection into tibia is also a method to create bone tumors. On the contrary, inoculation of lung cancer cells into the lung belongs to orthotopic models that are more relevant to naturally occurring lung cancer. The present study established in-house orthotopic or heterotopic xenograft models by establishing intrathoracic, intrabronchial, intracardiac, and intravenous models with various A549 cell lines. In addition, a subline derived from bone metastasis was tested in the intravenous model.

6.2 MATERIALS AND METHODS/RESULTS

Transfection: A549 cells were co-transfected with turboFP635 (Evrogren, Moscow, Russia) , a far-red fluorescent protein with luc2, a firefly luciferase (Promega, WI, USA). Lipofectamine^{TM} 2000 (Invitrogen, NY, USA) was used following the manufacture's instruction for transfection.

Animals: Male CD-1 athymic mice (6-8 weeks of age) were obtained from Charles River Laboratories (Wilmington, MA). The Principles of Animal Care by the National Institutes of Health (NIH) and a protocol approved by the Rutgers University Institutional Animal Care and Use Committee were complied to perform animal experiments. The animals were housed in an animal facility at the University, maintained on a 12-h light/dark cycle in a temperature-controlled environment, with food and water *ad libitum*.

Orthotopic NSCLC mouse model: Animals were anesthetized with ketamine and xylazine (80/12 mg/kg) by intraperitoneal injection. Then the mice were placed in the right lateral decubitus position. After disinfection, $2x10^6$ transfected A549RL cells (supendedin 0.03 ml medium containing 50% Matrigel®) were injected with a insulin syringe attached with a 28-gauge needle into the intercostal space at the dorsal mid-axillary line just below the inferior border of the scapula. Mice were turned to the left lateral decubitus position and kept warm to recover. The animals were then monitored daily, and body weigh was measurement weekly.

Regimen of ALA and CPT: CD-1 athymic mice injected with A549RL were anesthetized with isoflurane and injected with luciferin as luciferase substrate at day 5 after cell inoculation. The animals were then subjected to optical imaging (IVIS 100, Caliper Life Sciences) for the measurement of luminescence that reflected the tumor growth in the lung. Based on the total flux of photon, the animals were randomized into 4 groups at day 5 after cell inoculation (4 mice/group): control group, ALA group, CPT group, and combination group. ALA (200 mg/kg) was administered orally daily from day 5 after cell inoculation throughout the study. CPT- (2 mg CPT equivalent/kg) formulated as Vitamine E prodrug nanoparticles (150 nm) was dosed intravenously from day 7 twice

a week for 4 weeks. The lung tumor was monitored weekly by optical imaging. At termination of the study, the animals were further subjected to MRI and CT imaging to acquire lung tumor volume.

MRI and CT imaging: Animals were anesthetized under isoflurane during all imaging procedures. The CT scan was conducted with Albira high-resolution PET/ computed tomography scanner (Carestream Molecular Imaging, Woodbridge, CT). The scan parameters were set as follow: tube voltage 45 kVp, tube current 400μA, FOV 70 x 70 mm, detector pixels 2400 x 2400. Total scan duration was about 12 minutes. Image data were reconstructed using FBP algorithm. The resulting voxel size of the isotropic dataset was 125 microns. CT datasets were visualized using the software packages PMOD 3.3 (PMOD Technologies). T2 weighted MRI images (repetition time 2607 ms, echo time 44 ms) were recorded in Fast Spin Echo sequence using a 1 T M2™ whole body scanner (Aspect Imaging, 27 Hashaked St. Industrial Area Hevel Modi'in Shoham, 60850, Israel). At a spatial resolution of 312 micron, the tumors were coronal imaged in a single section through the lung using an image matrix of 256 × 256, a field of view of 80 mm^2, and 4 excitation. Tumor volume was calculated using Vivoquant 1.21.

Cell transfection: A549, a human NSCLC cell line, was purchased from ATCC (Manassas, VA). The cell line was maintained in Dulbecco's modified eagle's medium supplemented with 10% fetal bovine serum (FBS), penicillin (200 units/ml), and streptomycin (200 mg/ml) at 37 °C in 5% CO2 atmosphere. Cells with confluency less than 80% were used for animal inoculation. A549 cells were co-transfected with the

firefly luciferase (Luc2) and TurboFP635, a red fluorescence protein (RFP), using Lipofectamine 2000® (Invitrogen, Grand Island, NY) to deliver the vectors. Briefly, the cells were first transfected with pTurboFP635-N (Evrogen, Moscow, Russia) according to the manufacturer's instructions. Stably transfected clones were obtained by selection with neomycin. The RFP transfected cells were further transfected with GL4.50 {luc2/CMV/Hygro}vector (Promega, Madison, WI). Cells were thereafter selected with neomycin and hydromycin to obtain stably cotransfected clones (A549RL).

Microscopy: Cells or sections were examined with microscopy using Olympus IX71 microscope equipped with DP30BW and Infinity cameras. The conditions to capture images are indicated in the legends.

Animals: NOD.Cg-Prkdc^{scid} Il2rg^{tm1Wjl}/SzJ mice (NSG mice, stock number 005557) were purchased as breeders from The Jackson Laboratory (Bar Harbor, Maine). The mice were bred in Laboratory Animal Services at Rutgers, The State University of New Jersey, which is accredited by the Association for Assessment and Accreditation of Laboratory Animal Care International (AAALAC). CD-1 athymic mice were from Charles River Laboratories (Wilmington, MA). Mice at age of 10-12 weeks were used in the study. The animals were housed in pathogen-limited animal facility with free access to food and water. The light cycle was 12 hours in light and 12 hours in dark and the room temperature was maintained between 68 and 74ºF. All procedures involving mice were approved by the Institutional Animal Care and Use Committee.

Intrathoracic injection technique (IT model): This model is an orthotopic lung cancer model with 100% incidence of lung cancer onset. Mice anesthetized with isoflurane were

placed in the right lateral decubitus position. Insulin syringes (Becton Dickinson) with 31-gauge needles were used to inject the cell inoculum percutaneously into the left lateral thorax, at the lateral dorsal axillary line, 1.5 cm above the lower rib line just below the inferior border of the scapula. The needle was quickly advanced 5–6 mm into the thorax and was quickly removed after the injection of cell suspension. After tumor injection, the mouse was turned to the left lateral decubitus position. Animals were monitored until fully recovered. (Ref Amir Onn, Takeshi Isobe, Satoshi Itasaka, et al., Clin Cancer Res 2003;9:5532-5539). The technique was practiced and refined.

Histology: Animals were sacrificed by exsanguination under anesthesia. Formalin-inflated lung and other tissues were fixed with 10% neutrally buffered formalin for 24 hr. Fixed tissue were embedded with either paraffin or OCT compound (Sakura Finetek, Torrance, CA). Routine procedures were followed for paraffin embedding. As for OCT embedding, the tissues were cryopreserved with 30% sucrose solution prior to embedding step. Sections at thickness of 5 and 10 micron for paraffin and OCT blocks respectively were stained with hematoxylin and eosin (Sigma-Aldrich, St. Louis, MO).

In vivo optical imaging: The animals were administered with luciferin (150 mg/kg) intraperitoneally. Bioluminescence was captured using MS FX Pro (Bruker/CareStream, Rochester, NY) and Carestream Molecular Imaging Software MI (5.3.3). Luminescence, bright field, fluorescence, and X-ray imaging procedures were incorporated in the imaging protocols accordingly. After luminescence, bright field or fluorescence image acquisitions, X-ray image was captured at 35 KVP while the animals were kept in the chamber for anatomical location of the monitored signal.

MRI and CT imaging: Animals were anesthetized under isoflurane during all imaging procedures. The CT scan was conducted with Albira high-resolution PET/ computed tomography scanner (Carestream Molecular Imaging, Woodbridge, CT). The scan parameters were set as follow: tube voltage 45 kVp, tube current 400μA, FOV 70 x 70 mm, detector pixels 2400 x 2400. Total scan duration was about 12 minutes. Image data were reconstructed using FBP algorithm. The resulting voxel size of the isotropic dataset was 125 microns. CT datasets were visualized using the software packages PMOD 3.3 (PMOD Technologies). T2 weighted MRI images (repetition time 2607 ms, echo time 44 ms) were recorded in Fast Spin Echo sequence using a 1 T M2™ whole body scanner (Aspect Imaging, 27 Hashaked St. Industrial Area Hevel Modi'in Shoham, 60850, Israel). At a spatial resolution of 312 micron, the tumors were coronal imaged in a single section through the lung using an image matrix of 256 × 256, a field of view of 80 mm2, and 4 excitation.

Establishment of metastatic subline: A549RL injected intrathoracically into the left lung of CD-1 athymic mice. Some mice developed metastatic lesions in multiple organs such as bone, liver and brain. The organs were cut into small pieces and treated with collagenase type IV (StemCell Technologies Inc, Vancouver, Canada). The resulting suspensions were incubated under the selective condition to obtain sublines of A549RL. A subline from bone metastasis was selected for further studies.

Preliminary results of IT model: A549RL or the TS (subline derived from a bone metastatic lesion) were harvested by trypsinization or EDTA (2 mM) treatment. The cells were thereafter suspended in medium or Matrigel® for intrathoracic injection. NSG mice, both male female, at age of 12-14 weeks were injected following aforementioned procedures. Each point represents the mean ± SE of 7-9 animals. Primary tumor was developed over time. The subline exhibited a faster growth than the parent cell line. The metastatic incidence measured with optical imaging was about 20-30% in TS group.

Intracardiac injection technique (IC model):

Bone metastases are a common occurrence in lung cancer, which is responsible for significant morbidity and mortality. Several in vivo models have been established to study these events and each has specific benefits and limitations. The most commonly used model utilizes intracardiac inoculation of tumor cells directly into the arterial blood supply of immunodeficient mice[99].

Mice were anesthetized with isoflurane and the chest area was depilated with Nair. They were then placed at supine position and fixed by taping the forelimbs, and abdomen just below the xiphoid. The chest was disinfected with a betadine followed by cleaning with 70% ethanol for 3 times. Injection site was determined as the midway between the sternal notch and top of xiphoid process, and slightly left (anatomical) of the sternum. Syringes with 28G needle were used for cell injection. Successful insertion into left cardiac ventricle could be confirmed by distinct bright red pulse of blood into the syringe. Cells suspended in 0.1 ml PBS were carefully injected. After the injection, plunger was pulled up slightly to create a small amount of negative pressure to reduce

dripping of cells into the chest cavity. Gentle pressure was applied to the injection site reduce bleeding. The injected mice were then removed from the nose cone and continue to apply light pressure for about 1 min. They were monitored until fully conscious. The IC model achieved much faster tumor growth and high incidence of bone metastasis. More than half of the mice developed bone metastasis. In the low cell load group, there was a trend for higher incidence of spinal metastasis.

Intrabronchial intubation (IB model):

The mice were anesthetized with ketamine/xylazine (80/12 mg/kg) intraperitoneally and placed on a vertical support, suspended by its upper incisors. The tongue was gently pulled out, and the angle of the head was adjusted with holding fingers to expose the vocal cords. A house made intubation unit that included a fiber optic cable as a light source and introducer together with a 20G cannula, was then pushed through the visualized vocal cords for about 5 mm. harder on the tongue using the middle finger as support. The fiber optic cable was then withdrawn without moving the cannula. Cells suspended in 0.1 ml PBS containing EDTA (1 mM) were then injected through the cannula. The animals were then monitored until fully conscious.

Intravenous injection (IV model): A549RL and sublines were injected into NSG mice at cell load of $2x10^6$ per mouse.

MRI and CT Imaging:

Mice were placed in the isoflurane induction chamber at 4-5% isoflurane with an oxygen flow rate of 1 l/min. After the mouse was sedate, the isoflurane was adjusted to 1.5-2.0% depending on the mouse respiratory rate. The rate was maintained between 30-85 beats

per minute. The mouse was placed onto the imaging cradle in the prone position, with its mouth and nose locked into the isoflurane head-piece with a jaw lock bar. The cradle was then positioned so the mouse was in the center of the coil, then the mouse and cradle were placed into the MRI RAT Coil-60mm. For more specific scans of a limb, the Mouse-35mm coil will be used] Once the mouse was in the coil, a "Scout" scan was performed: This scan confirmed the positioning of the mouse in the MRI coil. Once the location was confirmed, a coil calibration was then performed. This calibration insured the frequency was correct. Thereafter a final calibration was performed. This calibration checked the RF pulse and other aspects of the MRI signals and scan. This same calibration was re-done after every 3 mice. If there was an image issue, the coil calibration was checked and adjusted. (Coil Calibration is normally only required once in the morning and once in the afternoon)

The scan for this study was the Fast Spin Echo, or FSE sequence using a 1 T M2™ whole body scanner (Aspect Imaging, 27 Hashaked St. Industrial Area Hevel Modi'in Shoham, 60850, Israel) . The scan was T2 weighted, which caused the tumors to be bright versus the background tissue. The scan was run on the Coronal Plane (versus Axial or Sagittal). Most of the scans were run with a slice package of 15 slices that were 1.5mm thick. (For smaller scans, we have used 0.5-1mm thick slices)0 The field of view was 100mm, which allowed for the scan of the entire mouse (missing some of the head/nose region). The scan was run at a 256-250 matrix, with the TE/TR at 80/2840 and a Flip Angle of 180 degrees. Four averages (with each average improving the image quality) were used in each scan. Average scan time was 5 minutes, adding 2 minutes per additional average when required. When the scan was completed, the mouse was

removed from the coil and cradle and placed back in its box. The box was then placed under a heating lamp while the mouse recovered.

The data was transferred from the MRI to an analysis software program Vivoquant®. In Vivoquant® the images were reviewed to look for any activity (lung tumors or fluid, enlarged spleen or lymph nodes, new metastasis).

6.3 DISCUSSION

The IT model is an orthotopic lung cancer model with primary tumor onset and moderate metastatic incidence. IC model is a fast tumor growing model with highest incidence of bone and liver metastasis. IB model is another orthotopic model and well published. However, development of the primary tumor seems to be very slow. Increasing cell load is not practical for large scale studies. IV injection of tumor cells is a traditional model to mimic extensive metastasis, but it also appears to be time consuming in our studies. Depending on the study perspectives, IT and IC models are considered as the top leads for practicality, time consideration, and relevance to human occurrence of NSCLC.

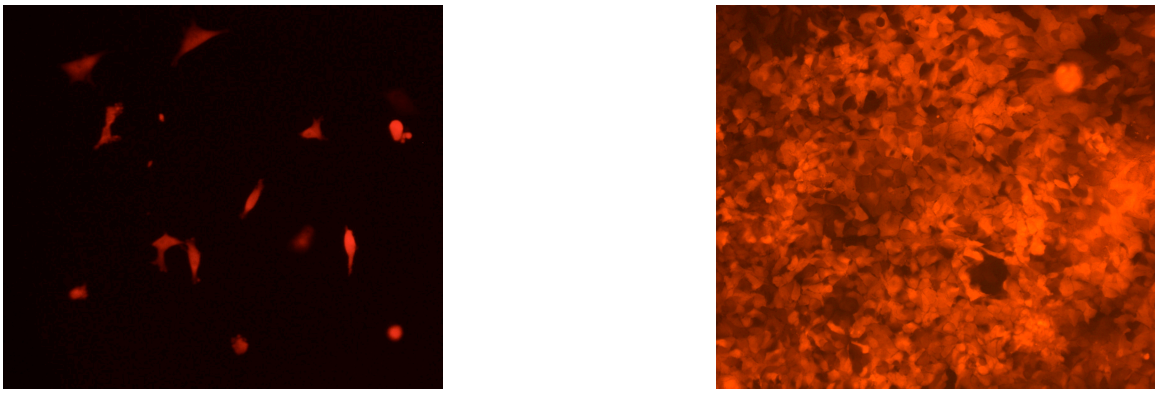

FIGURE 18 Fluorescence images of A549RL cells at low (left) and high (right) confluency. The images were captured using Olympus IX71 microscope equipped with an Infinity camera. Magnification: 100x; Filter: TRITC; Gain: 1.0; Shutter: 200 ms.

FIGURE 19 Left: NSG mouse; Right CD-1 athymic mouse

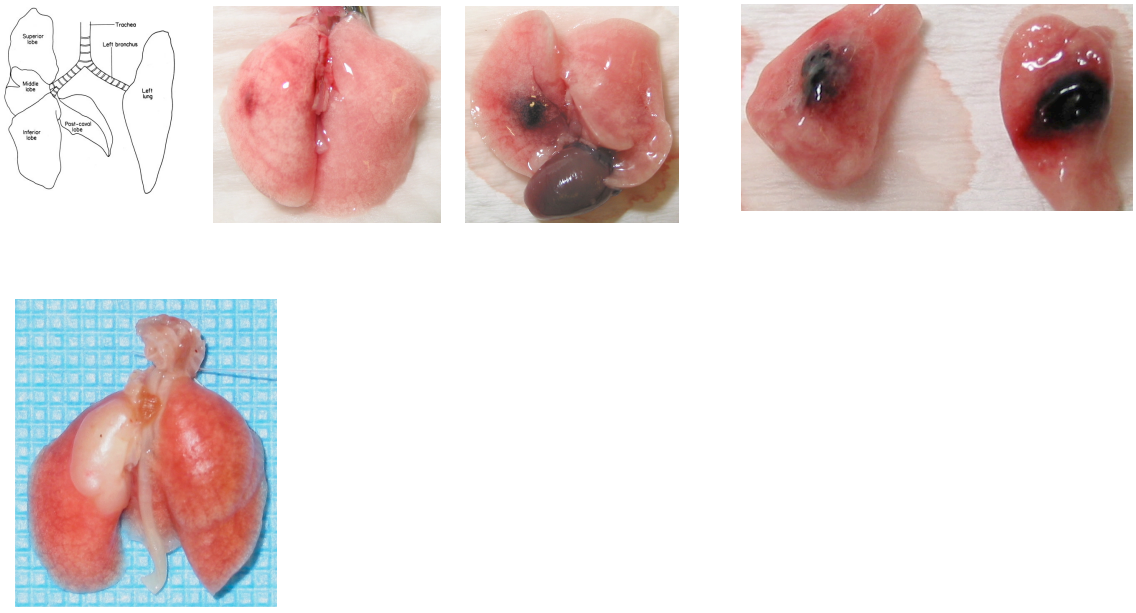

FIGURE 20

Top: 1) Mouse lung anatomy. Left lung was the injection target; 2) A successful injection with methylene blue into the left lung. About 0.03 ml of methylene blue (0.25%) suspended in Matrigel® (5 mg/ml) was injected. The mouse was sacrificed at 5 min after injection. Left & Middle: back and front view of the lung. Injection site and inoculum can be viewed. Right: the left lung was cut, displaying inoculum.

Bottom: A successful injection with A549 cells. A549 cells ($3x10^6$) suspended in Matrigel® were injected using the technique described. Tumor growth in the left lung is clearly shown.

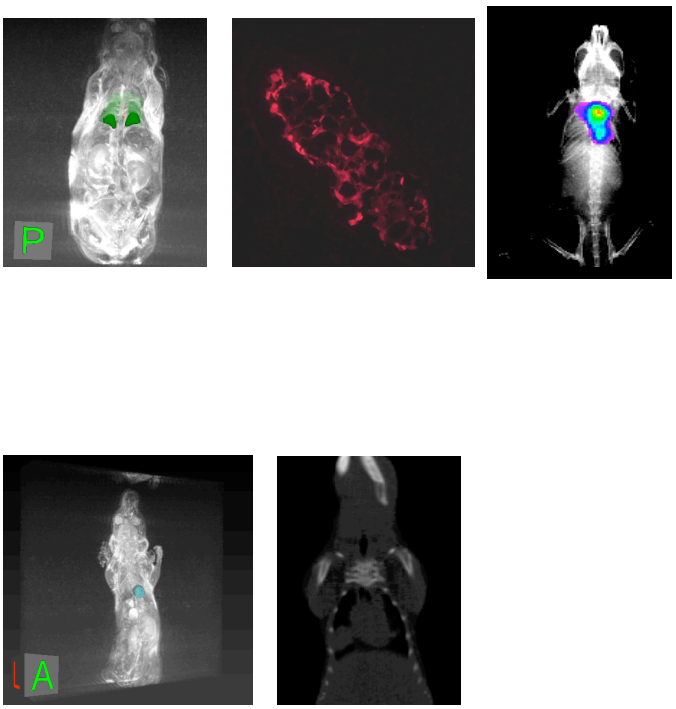

FIGURE 21 Validation of various imaging modalities for tumor detection.
Top left: an athymic mouse bearing A549RL tumors was imaged with MRI. Tumors (colored red) were observed in the left lung (whole lung colored green). Top right: fluorescence image of a lung cryosection of the mouse.
Bottom: A SCID mouse bearing lung tumor was imaged with FX Pro (left) on luminescence and X-ray; MRI (middle); and CT (right).

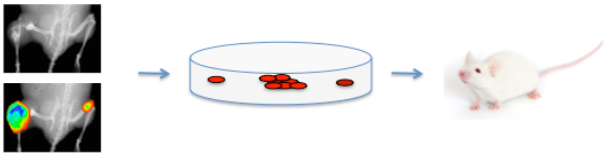

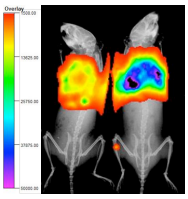

FIGURE 22 Establishment of metastatic sublines.

Top 1: Schematic process to isolate subclones from bone metastasis.

Top 2: a CD-1 athymic mouse showing bone metastasis. Left 1: co-registered image of luminescence and X-ray; Left 2: X-ray only, displaying severe bone destruction; Left 3: MRI image of metastatic lesions; Left 4: fluorescence microscopic image of a clone from the bone metastasis.

Top 3: Subline derived from the small bone metastasis was injected intrathoracically into NSG mice. Two mice are showing liver and bone metastasis in a pilot study.

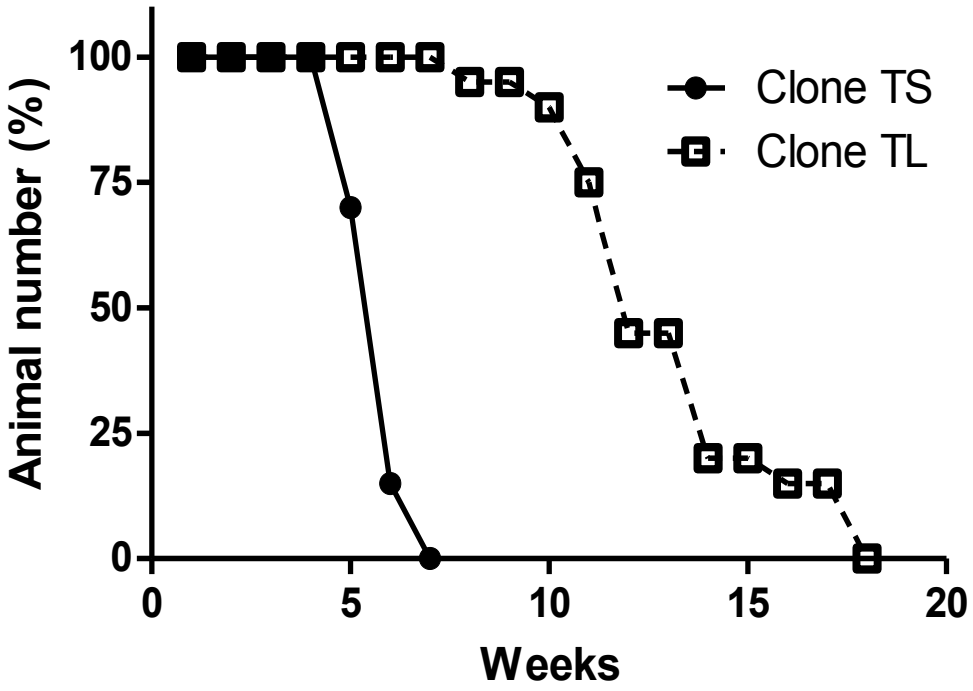

FIGURE 23 Comparison of two bone metastasis sublines (TS and TL, both from bone metastasis) in IT model. TS subline displayed much higher lethality in IT model than TL. Endpoint criteria were used for termination of animals.

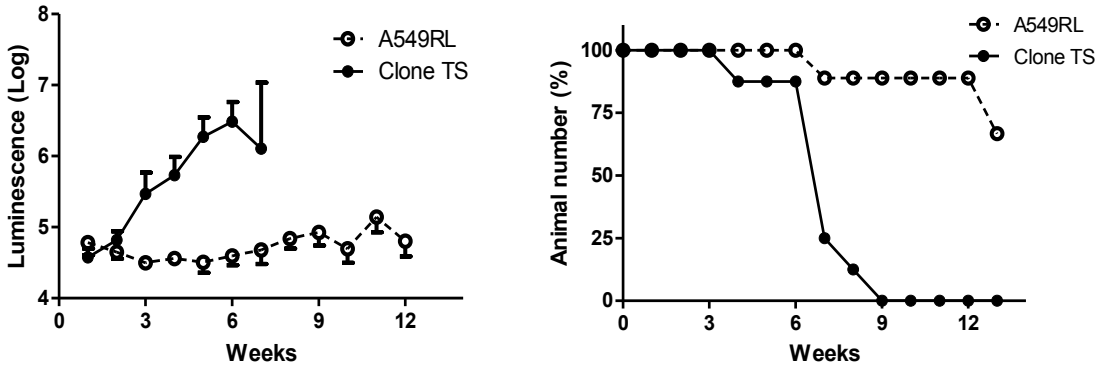

FIGURE 24 A549RL and subline clone TS were harvested with trypsinization and suspended in culture medium. The cells ($2x10^6$) were injected into the left lung intrachoracically as described above. Left, time course of lung tumor growth represented by luminescence. Mice were imaged weekly with FX Pro and luminescence from thorax was quantified. Each point represents the mean±SE (n=8-9). Right, time course of mouse number during lung tumor growth. Mice meeting endpoint criteria were euthanized.

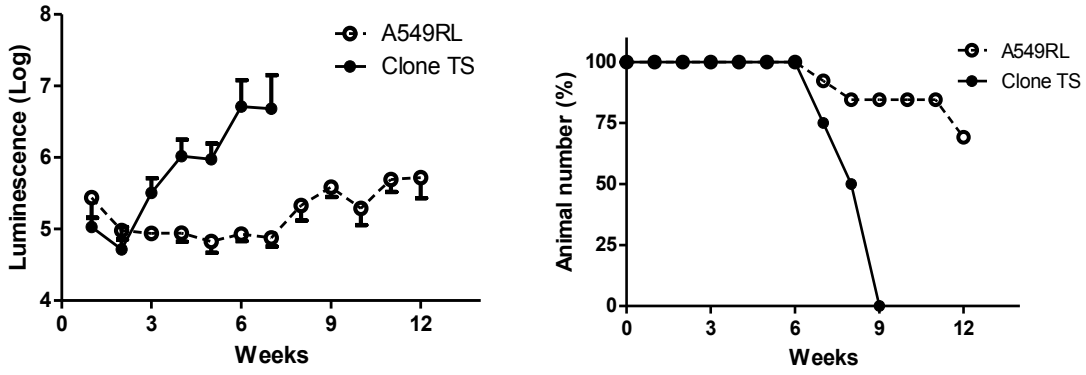

FIGURE 25 A549RL and subline Clone TS cells were harvested with trypsinization and resuspended in Matrigel. The cells ($2x10^6$) were injected into the left lung intrachoracically as described above. Left, time course of lung tumor growth. Mice were imaged weekly with FX Pro and luminescence was quantified. Each point represents the mean±SE (n=8-9). Right, time course of mouse number during lung tumor growth. Mice meeting endpoint criteria were euthanized.

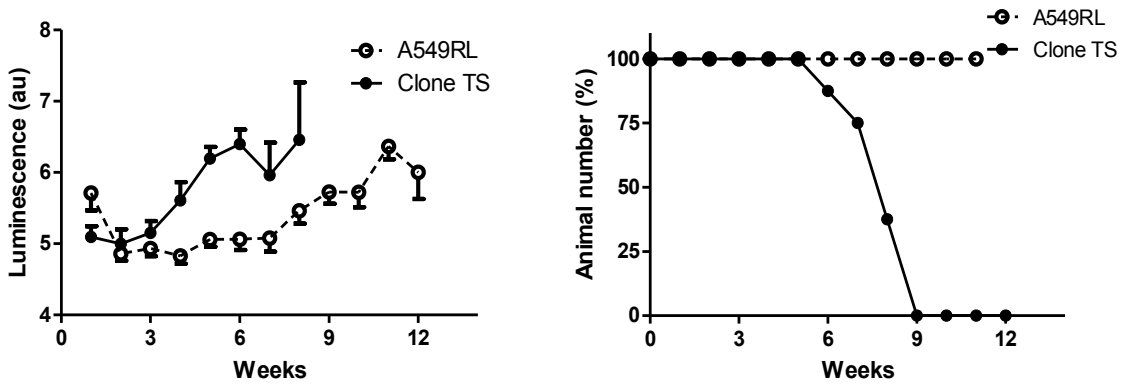

FIGURE 26 A549RL and subline Clone TS cells were harvested with EDTA (2 mM) and resuspended in Matrigel. The cells ($2x10^6$) were injected into the left lung intrachoracically as described above. Left, time course of lung tumor growth. Mice were imaged weekly with FX Pro and luminescence was quantified. Each point represents the mean±SE (n=8-9). Right, time course of mouse number during lung tumor growth. Mice meeting endpoint criteria were euthanized.

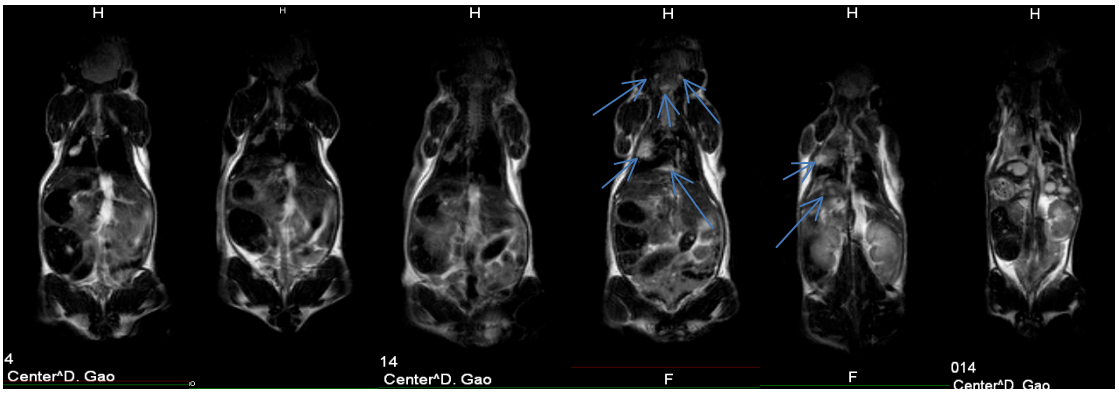

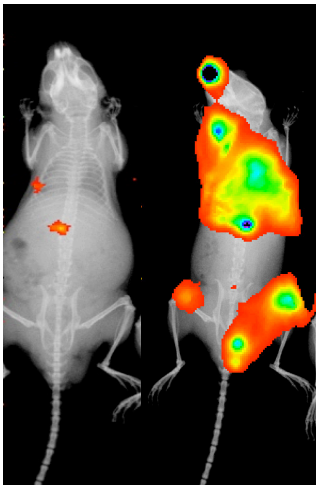

FIGURE 27 An example of time course of tumor growth in IT model by MRI scan and optical imaging. The mouse was inoculated with TS subline and monitored weekly. MRI images demonstrate primary tumor development over time and formation of distal metastasis (upper). Luminescence images show the same mouse at week 1 and six, in consistent with results of MRI (lower).

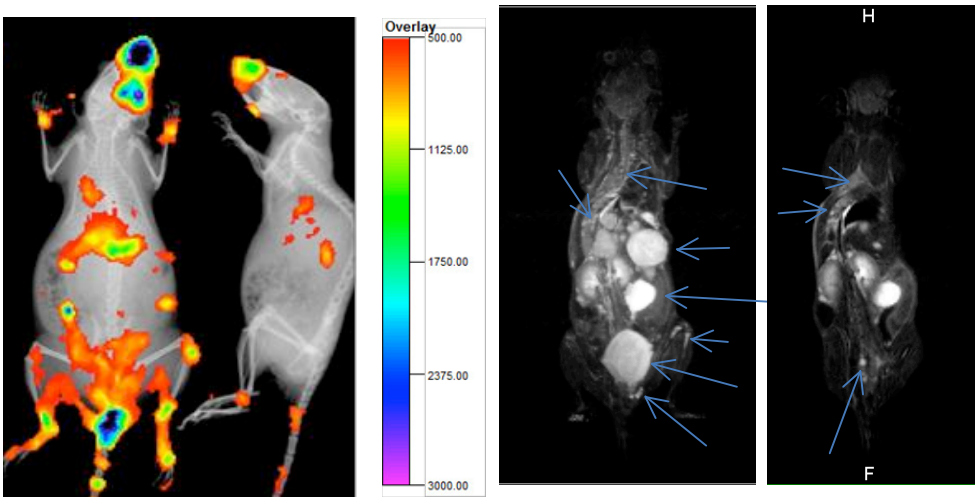

FIGURE 28 IC Model Various cell loads (10^5, 5x 10^5, and 2x 10^6 cells per mouse) were injected to test the development of metastasis in IC model. An example showing NSG mice injected via IC with 2x10^6 subline at week 1, demonstrating rapid distribution of cells in multiple sites (left). MRI images show metastatic lesions in mice inoculated with 10^5 cells at week 7 (middle and right).

FIGURE 29 IB Model Luminescence and MRI images of an intubated mouse at week 20 after inoculation. Subline was intubated at 5x106 cells in 0.1 ml PBS containing 1 mM. This model appeared to be a very slow development of primary tumor.

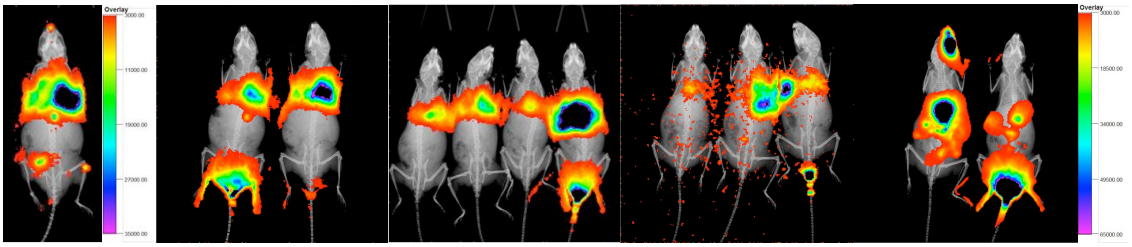

FIGURE 30 IV Model From left: A549RL at month 4, TS at week 9, Clone LR at week 9, Clone Br at week 9.

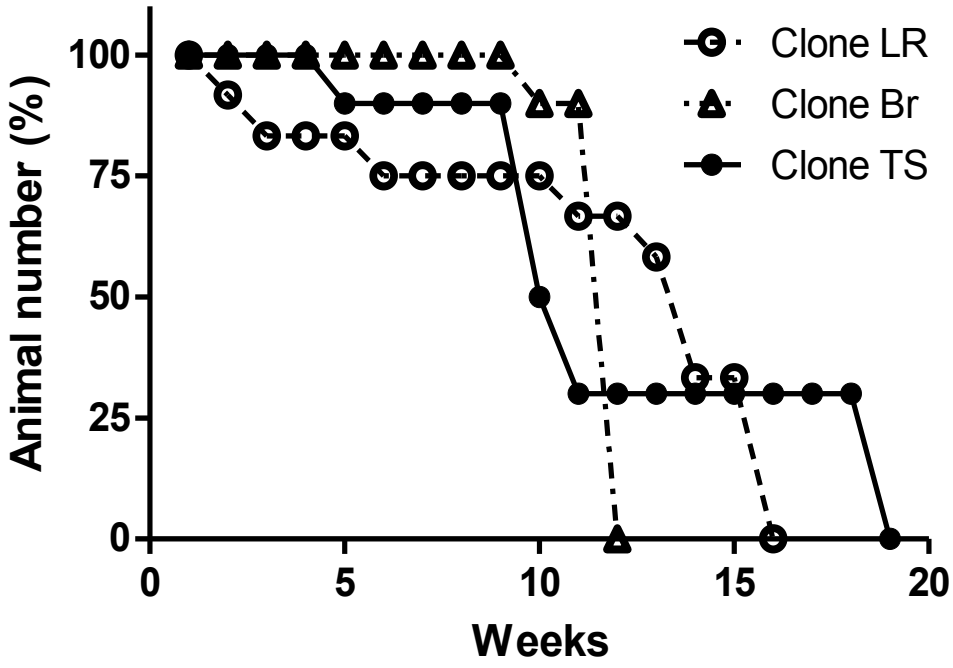

FIGURE 31 Animal survival graph of 3 sublines in IV model. TS and Clone LR were from bone metastasis, and Clone Br was from brain metastasis.

7. REFERENCES

1. Ferlay, J., et al., *Estimates of worldwide burden of cancer in 2008: GLOBOCAN 2008.* Int J Cancer. **127**(12): p. 2893-917.
2. Houlihan, N.G., et al., *Lung cancer*, in *Site-specific cancer series*. 2012, Oncology Nursing Society,: Pittsburgh, Pa.
3. Johnson, D.H., et al., *Randomized phase II trial comparing bevacizumab plus carboplatin and paclitaxel with carboplatin and paclitaxel alone in previously untreated locally advanced or metastatic non-small-cell lung cancer.* J Clin Oncol, 2004. **22**(11): p. 2184-91.
4. Pizzolato, J.F. and L.B. Saltz, *The camptothecins.* Lancet, 2003. **361**(9376): p. 2235-42.
5. Burke, T.G. and V.R. Adams, *Camptothecins in cancer therapy*. Cancer drug discovery and development. 2005, Totowa, N.J.: Humana Press. xiii, 460 p.
6. Choi, S.Y., J.H. Yu, and H. Kim, *Mechanism of alpha-lipoic acid-induced apoptosis of lung cancer cells.* Ann N Y Acad Sci, 2009. **1171**: p. 149-55.
7. Guais, A., et al., *Adding a combination of hydroxycitrate and lipoic acid (METABLOC) to chemotherapy improves effectiveness against tumor development: experimental results and case report.* Invest New Drugs.
8. Na, M.H., E.Y. Seo, and W.K. Kim, *Effects of alpha-lipoic acid on cell proliferation and apoptosis in MDA-MB-231 human breast cells.* Nutr Res Pract, 2009. **3**(4): p. 265-71.
9. Wenzel, U., A. Nickel, and H. Daniel, *alpha-Lipoic acid induces apoptosis in human colon cancer cells by increasing mitochondrial respiration with a concomitant O2-*-generation.* Apoptosis, 2005. **10**(2): p. 359-68.
10. Biewenga, G.P., G.R. Haenen, and A. Bast, *The pharmacology of the antioxidant lipoic acid.* Gen Pharmacol, 1997. **29**(3): p. 315-31.
11. Carlson, D.A., et al., *The plasma pharmacokinetics of R-(+)-lipoic acid administered as sodium R-(+)-lipoate to healthy human subjects.* Altern Med Rev, 2007. **12**(4): p. 343-51.
12. Links, M. and C. Lewis, *Chemoprotectants: a review of their clinical pharmacology and therapeutic efficacy.* Drugs, 1999. **57**(3): p. 293-308.
13. Smith, J.R., et al., *Differential activity of lipoic acid enantiomers in cell culture.* J Herb Pharmacother, 2005. **5**(3): p. 43-54.
14. Loffelhardt, S., et al., *Interaction of alpha-lipoic acid enantiomers and homologues with the enzyme components of the mammalian pyruvate dehydrogenase complex.* Biochem Pharmacol, 1995. **50**(5): p. 637-46.
15. Zimmer, G., et al., *Dose/response curves of lipoic acid R-and S-forms in the working rat heart during reoxygenation: superiority of the R-enantiomer in enhancement of aortic flow.* J Mol Cell Cardiol, 1995. **27**(9): p. 1895-903.
16. Ridge, C.A., A.M. McErlean, and M.S. Ginsberg, *Epidemiology of lung cancer.* Semin Intervent Radiol, 2013. **30**(2): p. 93-8.
17. Doll, R. and A.B. Hill, *Smoking and carcinoma of the lung. Preliminary report. 1950.* Bull World Health Organ, 1999. **77**(1): p. 84-93.
18. Samet, J.M., *Tobacco smoking: the leading cause of preventable disease worldwide.* Thorac Surg Clin, 2013. **23**(2): p. 103-12.

19. Bjerager, M., et al., *Delay in diagnosis of lung cancer in general practice.* Br J Gen Pract, 2006. **56**(532): p. 863-8.
20. Lang-Lazdunski, L., *Surgery for nonsmall cell lung cancer.* Eur Respir Rev, 2013. **22**(129): p. 382-404.
21. *Chemotherapy in non-small cell lung cancer: a meta-analysis using updated data on individual patients from 52 randomised clinical trials. Non-small Cell Lung Cancer Collaborative Group.* BMJ, 1995. **311**(7010): p. 899-909.
22. Forde, P.M. and D.S. Ettinger, *Targeted therapy for non-small-cell lung cancer: past, present and future.* Expert Rev Anticancer Ther, 2013. **13**(6): p. 745-58.
23. Alberg, A.J., et al., *Epidemiology of lung cancer: Diagnosis and management of lung cancer, 3rd ed: American College of Chest Physicians evidence-based clinical practice guidelines.* Chest, 2013. **143**(5 Suppl): p. e1S-29S.
24. Alberg, A.J., M.V. Brock, and J.M. Samet, *Epidemiology of lung cancer: looking to the future.* J Clin Oncol, 2005. **23**(14): p. 3175-85.
25. de Groot, P. and R.F. Munden, *Lung cancer epidemiology, risk factors, and prevention.* Radiol Clin North Am, 2012. **50**(5): p. 863-76.
26. Molina, J.R., et al., *Non-small cell lung cancer: epidemiology, risk factors, treatment, and survivorship.* Mayo Clin Proc, 2008. **83**(5): p. 584-94.
27. Dearden, S., et al., *Mutation incidence and coincidence in non small-cell lung cancer: meta-analyses by ethnicity and histology (mutMap).* Ann Oncol, 2013. **24**(9): p. 2371-6.
28. Cooper, W.A., et al., *Molecular biology of lung cancer.* J Thorac Dis, 2013. **5**(Suppl 5): p. S479-90.
29. Reungwetwattana, T. and G.K. Dy, *Targeted therapies in development for non-small cell lung cancer.* J Carcinog, 2013. **12**: p. 22.
30. Tomaszek, S.C. and D.A. Wigle, *Surgical management of lung cancer.* Semin Respir Crit Care Med, 2011. **32**(1): p. 69-77.
31. Lackey, A. and J.S. Donington, *Surgical management of lung cancer.* Semin Intervent Radiol, 2013. **30**(2): p. 133-40.
32. Carbone, D.P. and E. Felip, *Adjuvant therapy in non-small cell lung cancer: future treatment prospects and paradigms.* Clin Lung Cancer, 2011. **12**(5): p. 261-71.
33. Pennell, N.A., *Selection of chemotherapy for patients with advanced non-small cell lung cancer.* Cleve Clin J Med, 2012. **79 Electronic Suppl 1**: p. eS46-50.
34. Howington, J.A., et al., *Treatment of stage I and II non-small cell lung cancer: Diagnosis and management of lung cancer, 3rd ed: American College of Chest Physicians evidence-based clinical practice guidelines.* Chest, 2013. **143**(5 Suppl): p. e278S-313S.
35. Cohen, M.H., et al., *FDA drug approval summary: bevacizumab (Avastin) plus Carboplatin and Paclitaxel as first-line treatment of advanced/metastatic recurrent nonsquamous non-small cell lung cancer.* Oncologist, 2007. **12**(6): p. 713-8.
36. Govindan, R., *Summary of the proceedings from the 10th annual meeting of molecularly targeted therapy in non-small cell lung cancer.* J Thorac Oncol, 2010. **5**(12 Suppl 6): p. S433.

37. Hecht, S.S., F. Kassie, and D.K. Hatsukami, *Chemoprevention of lung carcinogenesis in addicted smokers and ex-smokers.* Nat Rev Cancer, 2009. **9**(7): p. 476-88.
38. Keith, R.L., et al., *Oral iloprost improves endobronchial dysplasia in former smokers.* Cancer Prev Res (Phila), 2011. **4**(6): p. 793-802.
39. Lynch, T.J., et al., *Ipilimumab in combination with paclitaxel and carboplatin as first-line treatment in stage IIIB/IV non-small-cell lung cancer: results from a randomized, double-blind, multicenter phase II study.* J Clin Oncol, 2012. **30**(17): p. 2046-54.
40. Mendelsohn, J. and Z. Fan, *Epidermal growth factor receptor family and chemosensitization.* J Natl Cancer Inst, 1997. **89**(5): p. 341-3.
41. Wang, H., et al., *Chemotherapy and chemosensitization of non-small cell lung cancer with a novel immunomodulatory oligonucleotide targeting Toll-like receptor 9.* Mol Cancer Ther, 2006. **5**(6): p. 1585-92.
42. Vinod, B.S., T.T. Maliekal, and R.J. Anto, *Phytochemicals as chemosensitizers: from molecular mechanism to clinical significance.* Antioxid Redox Signal, 2013. **18**(11): p. 1307-48.
43. Ren, H.Y. and X.W. Tang, *[Anti-proliferation and chemo-sensitization effects of apigenin on human lung cancer cells].* Zhejiang Da Xue Xue Bao Yi Xue Ban, 2011. **40**(5): p. 508-14.
44. Ko, J.C., et al., *Curcumin enhances the mitomycin C-induced cytotoxicity via downregulation of MKK1/2-ERK1/2-mediated Rad51 expression in non-small cell lung cancer cells.* Toxicol Appl Pharmacol, 2011. **255**(3): p. 327-38.
45. Khatri, N., et al., *cRGD Grafted siRNA Nano-constructs for Chemosensitization of Gemcitabine Hydrochloride in Lung Cancer Treatment.* Pharm Res, 2014.
46. Sen, Z., et al., *Chemosensitizing activities of cyclotides from Clitoria ternatea in paclitaxel-resistant lung cancer cells.* Oncol Lett, 2013. **5**(2): p. 641-644.
47. Lara, P.N., Jr., et al., *High-dose toremifene as a cisplatin modulator in metastatic non-small cell lung cancer: targeted plasma levels are achievable clinically.* Cancer Chemother Pharmacol, 1998. **42**(6): p. 504-8.
48. Jin, X., et al., *Chemosensitization in non-small cell lung cancer cells by IKK inhibitor occurs via NF-kappaB and mitochondrial cytochrome c cascade.* J Cell Mol Med, 2009. **13**(11-12): p. 4596-607.
49. Fiebiger, W., et al., *In vitro cytotoxicity of novel platinum-based drugs and dichloroacetate against lung carcinoid cell lines.* Clin Transl Oncol. **13**(1): p. 43-9.
50. Michelakis, E.D., L. Webster, and J.R. Mackey, *Dichloroacetate (DCA) as a potential metabolic-targeting therapy for cancer.* Br J Cancer, 2008. **99**(7): p. 989-94.
51. Papandreou, I., T. Goliasova, and N.C. Denko, *Anticancer drugs that target metabolism: Is dichloroacetate the new paradigm?* Int J Cancer. **128**(5): p. 1001-8.
52. Tong, J., et al., *Synergistic antitumor effect of dichloroacetate in combination with 5-fluorouracil in colorectal cancer.* J Biomed Biotechnol. **2011**: p. 740564.
53. Walker, S., *Updates in non-small cell lung cancer.* Clin J Oncol Nurs, 2008. **12**(4): p. 587-96.

54. Dempke, W.C., T. Suto, and M. Reck, *Targeted therapies for non-small cell lung cancer.* Lung Cancer. **67**(3): p. 257-74.
55. Ghibu, S., et al., *Antioxidant properties of an endogenous thiol: Alpha-lipoic acid, useful in the prevention of cardiovascular diseases.* J Cardiovasc Pharmacol, 2009. **54**(5): p. 391-8.
56. Goraca, A., et al., *Lipoic acid - biological activity and therapeutic potential.* Pharmacol Rep. **63**(4): p. 849-58.
57. Vallianou, N., A. Evangelopoulos, and P. Koutalas, *Alpha-lipoic Acid and diabetic neuropathy.* Rev Diabet Stud, 2009. **6**(4): p. 230-6.
58. Bustamante, J., et al., *Alpha-lipoic acid in liver metabolism and disease.* Free Radic Biol Med, 1998. **24**(6): p. 1023-39.
59. Suzuki, Y.J., B.B. Aggarwal, and L. Packer, *Alpha-lipoic acid is a potent inhibitor of NF-kappa B activation in human T cells.* Biochem Biophys Res Commun, 1992. **189**(3): p. 1709-15.
60. Dozio, E., et al., *The natural antioxidant alpha-lipoic acid induces p27(Kip1)-dependent cell cycle arrest and apoptosis in MCF-7 human breast cancer cells.* Eur J Pharmacol. **641**(1): p. 29-34.
61. Ho, Y.S., et al., *Dihydrolipoic acid inhibits skin tumor promotion through anti-inflammation and anti-oxidation.* Biochem Pharmacol, 2007. **73**(11): p. 1786-95.
62. Abolhassani, M., et al., *Screening of well-established drugs targeting cancer metabolism: reproducibility of the efficacy of a highly effective drug combination in mice.* Invest New Drugs.
63. Isidoro, A., et al., *Alteration of the bioenergetic phenotype of mitochondria is a hallmark of breast, gastric, lung and oesophageal cancer.* Biochem J, 2004. **378**(Pt 1): p. 17-20.
64. Warburg, O., *[The reaction of ascites tumor cells to oxygen under high pressure].* Arch Geschwulstforsch, 1953. **6**(1): p. 7-11.
65. Warburg, O., *[Origin of cancer cells].* Oncologia, 1956. **9**(2): p. 75-83.
66. Korotchkina, L.G., S. Sidhu, and M.S. Patel, *R-lipoic acid inhibits mammalian pyruvate dehydrogenase kinase.* Free Radic Res, 2004. **38**(10): p. 1083-92.
67. Mervaala, E., et al., *Lipoic acid supplementation prevents angiotensin II-induced renal injury.* Kidney Int, 2003. **64**(2): p. 501-8.
68. O'Brien, M., J. Eckardt, and R. Ramlau, *Recent advances with topotecan in the treatment of lung cancer.* Oncologist, 2007. **12**(10): p. 1194-204.
69. Deshmukh, M., et al., *A series of alpha-amino acid ester prodrugs of camptothecin: in vitro hydrolysis and A549 human lung carcinoma cell cytotoxicity.* J Med Chem. **53**(3): p. 1038-47.
70. Chao, P., et al., *Pulmonary targeting microparticulate camptothecin delivery system: anticancer evaluation in a rat orthotopic lung cancer model.* Anticancer Drugs. **21**(1): p. 65-76.
71. Lalloo, A., et al., *Pharmacokinetic and pharmacodynamic evaluation of a novel in situ forming poly(ethylene glycol)-based hydrogel for the controlled delivery of the camptothecins.* J Control Release, 2006. **112**(3): p. 333-42.
72. Paranjpe, P.V., et al., *Tumor-targeted bioconjugate based delivery of camptothecin: design, synthesis and in vitro evaluation.* J Control Release, 2004. **100**(2): p. 275-92.

73. Paranjpe, P.V., S. Stein, and P.J. Sinko, *Tumor-targeted and activated bioconjugates for improved camptothecin delivery.* Anticancer Drugs, 2005. **16**(7): p. 763-75.
74. Chou, T.C., *Drug combination studies and their synergy quantification using the Chou-Talalay method.* Cancer Res, 2010. **70**(2): p. 440-6.
75. Yoon, M.J., et al., *Superoxide anion and proteasomal dysfunction contribute to curcumin-induced paraptosis of malignant breast cancer cells.* Free Radic Biol Med. **48**(5): p. 713-26.
76. Das, A., N.L. Banik, and S.K. Ray, *Flavonoids activated caspases for apoptosis in human glioblastoma T98G and U87MG cells but not in human normal astrocytes.* Cancer. **116**(1): p. 164-76.
77. Manson, M.M., et al., *Innovative agents in cancer prevention.* Recent Results Cancer Res, 2005. **166**: p. 257-75.
78. Yamasaki, M., et al., *Dihydro-alpha-lipoic acid has more potent cytotoxicity than alpha-lipoic acid.* In Vitro Cell Dev Biol Anim, 2009. **45**(5-6): p. 275-80.
79. Minko, T., et al., *Enhancing the anticancer efficacy of camptothecin using biotinylated poly(ethylene glycol) conjugates in sensitive and multidrug-resistant human ovarian carcinoma cells.* Cancer Chemother Pharmacol, 2002. **50**(2): p. 143-50.
80. Lalloo, A.K., et al., *Membrane transport of camptothecin: facilitation by human P-glycoprotein (ABCB1) and multidrug resistance protein 2 (ABCC2).* BMC Med, 2004. **2**: p. 16.
81. Hanahan, D. and R.A. Weinberg, *The hallmarks of cancer.* Cell, 2000. **100**(1): p. 57-70.
82. Hanahan, D. and R.A. Weinberg, *Hallmarks of cancer: the next generation.* Cell, 2011. **144**(5): p. 646-74.
83. Pinkerton, N.M., et al., *Gelation chemistries for the encapsulation of nanoparticles in composite gel microparticles for lung imaging and drug delivery.* Biomacromolecules, 2014. **15**(1): p. 252-61.
84. Lee, H.S., M.H. Na, and W.K. Kim, *alpha-Lipoic acid reduces matrix metalloproteinase activity in MDA-MB-231 human breast cancer cells.* Nutr Res, 2010. **30**(6): p. 403-9.
85. Spano, D., et al., *Molecular networks that regulate cancer metastasis.* Semin Cancer Biol, 2012. **22**(3): p. 234-49.
86. Roninson, I.B., *Tumor cell senescence in cancer treatment.* Cancer Res, 2003. **63**(11): p. 2705-15.
87. Roninson, I.B., *Tumor senescence as a determinant of drug response in vivo.* Drug Resist Updat, 2002. **5**(5): p. 204-8.
88. Stock, A.M., et al., *Targets for anti-metastatic drug development.* Curr Pharm Des, 2013. **19**(28): p. 5127-34.
89. Wong, M.S., et al., *Molecular targets in the discovery and development of novel antimetastatic agents: current progress and future prospects.* Clin Exp Pharmacol Physiol, 2013. **40**(5): p. 307-19.
90. Bellou, S., et al., *Anti-angiogenesis in cancer therapy: Hercules and hydra.* Cancer Lett, 2013. **338**(2): p. 219-28.

91. Samant, R.S. and L.A. Shevde, *Recent advances in anti-angiogenic therapy of cancer.* Oncotarget, 2011. **2**(3): p. 122-34.
92. Ibrahim, S., D. Gao, and P.J. Sinko, *Selective cytotoxicity and combined effects of camptothecin or paclitaxel with sodium-R-alpha lipoate on A549 human non-small cell lung cancer cells.* Nutr Cancer, 2014. **66**(3): p. 492-9.
93. Lemaitre, V. and J. D'Armiento, *Matrix metalloproteinases in development and disease.* Birth Defects Res C Embryo Today, 2006. **78**(1): p. 1-10.
94. Vihinen, P. and V.M. Kahari, *Matrix metalloproteinases in cancer: prognostic markers and therapeutic targets.* Int J Cancer, 2002. **99**(2): p. 157-66.
95. Iizasa, T., et al., *Elevated levels of circulating plasma matrix metalloproteinase 9 in non-small cell lung cancer patients.* Clin Cancer Res, 1999. **5**(1): p. 149-53.
96. Ewald, J.A., et al., *Therapy-induced senescence in cancer.* J Natl Cancer Inst, 2010. **102**(20): p. 1536-46.
97. Kim, C.F., et al., *Mouse models of human non-small-cell lung cancer: raising the bar.* Cold Spring Harb Symp Quant Biol, 2005. **70**: p. 241-50.
98. Meuwissen, R. and A. Berns, *Mouse models for human lung cancer.* Genes Dev, 2005. **19**(6): p. 643-64.
99. Arguello, F., R.B. Baggs, and C.N. Frantz, *A murine model of experimental metastasis to bone and bone marrow.* Cancer Res, 1988. **48**(23): p. 6876-81.